SLAC-PUB-2068
December 1977

Charmed Particle Spectroscopy*

G.J. Feldman
Stanford Linear Accelerator Center
Stanford University, Stanford, Calif. 94305

I. Introduction

These lectures[1] will attempt to review what we have learned about charmed particles in the little over a year since they were definitively identified.[2,3] The recent discovery of the $\psi(3772)$[4,5] has given us a powerful tool for the detailed study of D mesons. By studying its decays we have been able to measure D meson masses and absolute branching ratios with an accuracy that only a few months earlier had been though to be beyond our reach. Accordingly, the emphasis of these talks will be on this recent work.

Figure 1 shows the ratio R of the total hadronic cross section to the muon pair production cross section in the threshold regions for charmed meson production.[4,6] Most of the work on charmed mesons has been done at the prominent peaks at 3.77, 4.03, and 4.41 GeV. The $\psi(3772)$ (or ψ'') is just above $D\bar{D}$ threshold and below $D\bar{D}^*$ threshold. The peak at 4.03 is just above $D^*\bar{D}^*$ threshold.

Section II will discuss the accurate determination of D meson masses and their consequences. Section III will cover the determination of D meson branching fractions for hadronic decay modes and their use in measuring the amount of charm production in e^+e^- annihilation at various energies. Semileptonic D meson branching ratios will be the subject of Section IV. Section V will explore some of the uses of tagged decays at the $\psi(3772)$. Sections VI and VII will cover D meson spin and parity determinations and the study of D^o-$\bar{D}^o$ mixing. Finally Sections VIII and IX will discuss what little is known about F mesons and charmed baryons.

*Work supported by the Department of Energy

(Lectures given at the Banff Summer Institute on Particles and Fields, Banff, Alberta, Canada, August 26 - September 3, 1977)

II. Masses

A. D^o and D^+ Masses

To calculate a mass one uses the formula

$$m = (E^2 - p^2)^{\frac{1}{2}} \quad . \tag{1}$$

The advantage of studying $e^+e^- \to D\bar{D}$ is that the energy E must equal E_b, the energy of one of the incident beams. E_b has an rms spread, due to quantum fluctuations in synchrotron radiation, of only about 1 MeV,[7] and its central value can be monitored to high precision.[8] For $D\bar{D}$ production near threshold, as in ψ' decays, we have the additional advantage that p^2 is small, about 0.08 $(GeV/c)^2$. Thus any error in p is demagnified in its effect on the determination of the mass. The final result is that we measure masses in ψ'' decays with an rms resolution of about 3 MeV/c^2, which is a factor of 5 to 10 better than they can be measured at higher energies.

In the SPEAR Magnetic Detector charged kaons are identifed by time-of-flight measurements[2,3] and neutral kaons are identified by measurement of the dipion mass and the consistency of the dipion vertex with the assumed kaon decay.[9] For each particle combination we first require that the measured energy agree with E_b to within 50 MeV and then calculate the mass from Eq. 1 with $E = E_b$. The results,[10] given in Fig. 2 in 4 MeV/c^2 wide bins, show clear signals in five modes including the previously unreported mode $D^- \to K_s^0\pi^-$. Figure 3 shows the D^+ and D^o mass spectra for the sum of all observed modes in 2 MeV/c^2 bins. The mass difference of about 5 MeV/c^2 between the D^+ and D^o is clearly visible. Fits to the mass spectra give

$$M_{D^o} = 1863.3 \pm 0.9 \text{ MeV}/c^2 \tag{2}$$

and

$$M_{D^+} = 1868.3 \pm 0.9 \text{ MeV}/c^2 \quad . \tag{3}$$

The errors are dominated by systematic uncertainties such as the absolute momentum calibration and the stability of E_b monitoring. The D^+-D^o mass difference is determined to be 5.0 ± 0.8 MeV/c^2; it is known more precisely than either D mass because several systematic errors cancel in the mass difference. The theoretical estimate of this mass difference has been widely discussed with estimates ranging from 2 to 15 MeV/c^2.[11]

B. D^{*o} Mass

To obtain the D^{*o} mass we employ the same trick with $D^{*o}\overline{D^{*o}}$ production at 4.028 GeV with the following differences:

a) We observe the D^o from $D^{*o} \to D^o\pi^o$ decay. Since the Q value of the reaction is small, the D^o carries off most of the D^{*o} momentum. Thus the detection of the D^o rather than the D^{*o} causes no real problem.

b) There is contamination from $D^{*+} \to D^o\pi^+$ and $D^{*o} \to D^o\gamma$ decays. Figure 4a shows the contributions to the D^o momentum spectrum. The problem here is to determine the center of peak $B[D^{*o} \to D^o\pi^o]$ in the presence of peaks $A[D^{*+} \to D^o\pi^+]$ and $C[D^{*o} \to D^o\gamma]$.

The data and a fit to the data are shown in Fig. 4b.[12] The D^{*o} mass is determined to be 2006 ± 1.5 MeV/c^2. The uncertainty is larger here than it was for the D^o or D^+ because of the difficulty of extracting the signal and because the fit is not perfect.

C. D^{*+} Mass

There are insufficient statistics to enable us to observe $D^{*+}D^{*-}$ production at 4.028 GeV (see Fig. 4c), so another method is used to obtain the D^{*+} mass: We observe the $D^{*+} \to D^o\pi^+$ decay directly. Since the Q value is small the π^+ momentum will be only m_π/m_{D^*} ($\approx$7%) of the D^* momentum. It is thus necessary to use high momentum D^*'s from high energy data ($E_{c.m.}$ = 6.8 GeV) to obtain pions with enough momentum to be visible in the magnetic detector.

The kinematics in this case are not as transparent as they were in the previous cases, but the essential point is that the Q value determines the kinematics and even a crude measurement of the Q value translates into a very precise measurement of the D^{*+} mass. Figure 5 shows the $D^{*+}-D^{o}$ mass difference in 1 MeV/c^2 bins.[13] The Q value is determined to be 5.7 $\pm$ 0.5 MeV which, when combined with the D^{o} mass, yields a D^{*+} mass of 2008.6 $\pm$ 1.0 MeV/c^2.

D. Mass Differences and Q Values

We previously gave the mass difference

$$\delta \equiv m_{D^+} - m_{D^o} = 5.0 \pm 0.8 \text{ MeV}/c^2 \quad . \tag{4}$$

We can now add

$$\delta^* \equiv m_{D^{*+}} - m_{D^{*o}} = 2.6 \pm 1.8 \text{ MeV}/c^2 \tag{5}$$

and

$$\delta - \delta^* = 2.4 \pm 2.4 \text{ MeV}/c^2 \tag{6}$$

The quantity $\delta-\delta^*$ is an electromagnetic hyperfine splitting for which theoretical estimates vary between 0 and 3 MeV/c^2.[11] The error given in Eq. 6 is somewhat larger than would be naively expected from Eqs. 4 and 5 due to correlations in the errors.

The Q values for $D^* \to D\pi$ and $D^* \to D\gamma$ are given in Fig. 6. The decay $D^{*o} \to D^+\pi^-$ appears to be kinematically forbidden in the limit of zero D^{*o} width. Even allowing for finite D^* width, it cannot be an important decay mode.

E. D^* Branching Fractions

The D^{*o} branching fractions have been determined from the D^o momentum spectrum at 4.028 GeV by fitting the relative contributions of curves B and C in Fig. 4a.[12] The result is $B(D^{*o} \to D^o\gamma) = 0.45 \pm 0.15$.[14] The D^{*+} branching fractions were not well determined from the 4.028 GeV data due to insufficient statistics, but we can now calculate them using the $D^* \to D\pi$ Q values and a few reasonable assumptions.

The inputs are:

a) D and D^* masses, and

b) $B(D^{*o} \to D^o\gamma)$.

The assumptions are:

a) Isospin conservation in $D^* \to D\pi$ decays,

b) $\Gamma(D^* \to D\pi)$ is proportional to p^3 where p is the D momentum in the rest frame, and

c) the quark model prediction for $\Gamma(D^* \to D\gamma)$:[15]

$$\frac{\Gamma(D^{*+} \to D^+\gamma)}{\Gamma(D^{*o} \to D^o\gamma)} = \frac{(\mu_c - \mu_{\bar{d}})^2}{(\mu_c - \mu_{\bar{u}})^2} \quad , \tag{7}$$

where μ is a quark magnetic moment which we assume is inversely proportional to the quark mass. Thus,

$$\frac{\Gamma(D^{*+} \to D^+\gamma)}{\Gamma(D^{*o} \to D^o\gamma)} = \left(\frac{2\frac{m_u}{m_c} - 1}{2\frac{m_u}{m_c} + 2} \right)^2 \tag{8}$$

taking $m_d = m_u$. The quark masses are not real masses and cannot be determined with any real accuracy. We will thus take two extreme cases to test the sensitivity of this assumption: $m_u/m_c = m_\rho/m_\psi$ and $m_u/m_c = 0$. We obtain

$$\frac{\Gamma(D^{*+} \to D^+\gamma)}{\Gamma(D^{*o} \to D^o\gamma)} = \begin{cases} 1/25 \text{ for } \frac{m_u}{m_c} = \frac{m_\rho}{m_\psi} \\ 1/4 \text{ for } \frac{m_u}{m_c} = 0 \end{cases} . \tag{9}$$

The results are given in Table I. Independent of the details of assumption (c), $B(D^{*+} \to D^+\gamma)$ is small, and $B(D^{*+} \to D^o\pi^+)$ is about twice as large as $B(D^{*+} \to D^+\pi^o)$. By accident, the total D^{*o} width is about equal to the D^{*+} width. The best experimental information on D^* widths

comes from Fig. 5 from which we can deduce that $\Gamma_{D^{*+}} < 2.0$ MeV/c^2 at the 90% confidence level.[13]

III. Branching Fractions into Hadronic Decay Modes

A. Modes With All Charged Particles

The cross section times branching fractions ($\sigma \cdot B$) for inclusive D production in various modes involving only charged particles have been determined at $E_{c.m.} = 3.774$, 4.028, and 4.414 GeV. The data from the ψ'' (i.e. 3.774 GeV) are shown in Fig. 2 and the data from 4.028 and 4.414 GeV are shown in Fig. 7.[16] The results are given in Table II.[17] The relative D^o branching fractions from 3.774 GeV and 4.028 GeV are in good agreement. The data from 4.414 GeV are not in as good agreement, but as can be seen from Fig. 7, there are higher backgrounds at 4.414 GeV than at lower energies and it is more difficult to extract the signal. No conclusive evidence for Cabbibo suppressed decays has been seen at any energy. There are upper limits given in Table II for $E_{c.m.} = 4.028$ GeV which are consistent with the expected degree of suppression.

B. Modes With a π^o

The addition of a wall of lead-glass blocks (LGW)[18] to the SPEAR Magnetic Detector allows us to search for D hadronic decay modes containing a π^o.[19] The LGW subtends about 10% of the solid angle covered by the detector's spark chambers and counters, as is shown in Fig. 8.

Figure 9a shows the reconstructed $\gamma\gamma$ mass spectrum for minimum γ momentum of 100 and 150 MeV/c. The π^o signal is clearly visible in both cases, although the mass resolution is poor for low energy photons which can lose a large fraction of their energy in the aluminum solenoid coil which preceeds the LGW. The acceptance for π^o's in the LGW is shown in Fig. 9b. At 600 MeV/c, the region of interest for D decays, the acceptance is about 1%.

Photon pairs detected in the LGW at the ψ'' are combined with charged particles found in the detector and the combination is fit with two constraints: that the total reconstructed energy equal the beam energy and that the $\gamma\gamma$ invariant mass equal the π^o masss. The invariant mass spectrum for $K^{\pm}\pi^{\mp}\pi^o$ combinations which given acceptable fits is shown in Fig. 10. A signal of 7.3 events over an estimated background of 1.7 events is seen at the D^o mass. This corresponds to a $\sigma \cdot B$ of 1.4 ± 0.6 nb.

No significant signals are seen in other possible decay modes. The upper limit on $\sigma \cdot B$ for $D^o \to \overline{K^o}\pi^o$ plus $\overline{D^o} \to K^o\pi^o$ is 0.7 nb at the 90% confidence level.

C. Absolute Branching Fractions

In the ψ'' we have for the first time a situation in which charm production is sufficiently simple that we can use measurements of the total cross section and of $\sigma \cdot B$ for D decay modes to calculate absolute branching fractions.

The inputs are

a) $\sigma \cdot B$ measurements at the ψ'' which we have just discussed, and

b) the total cross section measurements in the vicinity of the ψ''.[4]

The assumptions are

a) The ψ'' is a state of definite isospin, either 0 or 1. This assumption gives equal partial widths to $D^o\overline{D^o}$ and D^+D^- except for phase space factors.

b) The phase space factors are given by

$$\frac{p^3}{1 + (rp)^2} \qquad (10)$$

where p is the D momentum and r is an interaction radius.[20] The value of r is not known,[21] but as r varies from 0 to infinity, the fraction of $D^o\overline{D^o}$ changes from 0.59 to 0.53. We can thus take this fraction to be 0.56 ± 0.03. The error due to the uncertainty in r is small compared to other systematic errors.

c) $D\bar{D}$ is the only substantial decay mode of the ψ''. The rationale for this assumption is that the ψ' and ψ'' differ in mass by only 88 MeV/c^2 and thus should have similar decay modes to channels which are open to both states. However, the total ψ'' width is two orders of magnitude larger than the ψ' width. The most reasonable explanation for the difference in widths is to attribute most of the ψ'' width to the $D\bar{D}$ channel, which is accessible to it, but not to the ψ'. This is a dramatic example of the Okubo-Zweig-Iizuka rule.

The results are given in Table III. The $\bar{K}^0\pi^+$ decay mode of the D^+ is comparable in size to the $D^0 \to K^-\pi^+$ decay mode. This decay does not appear to be suppressed as was suggested from the analogue of octet enhancement in strangeness changing decays.[22]

D. Comparison to the Statistical Model

It is instructive to compare the absolute branching fractions given in Table III to the predictions of a statistical model. This model, due to Rosner,[23] uses a Poisson multiplicity distribution and, within each multiplicity, equal contributions from each isospin amplitude. There is no real theoretical justification for this model and one should probably view its predictions with a certain degree of skepticism. Nevertheless, it can serve as a crude guide to the reasonableness of the measurements.

The statistical model predictions are given in terms of the ratio of a given state to the sum of all states of the form $K + n\pi$. Therefore we will define $f_{Kn\pi}$ to be the ratio

$$f_{Kn\pi} = \frac{\Sigma B(D \to K + n\pi)}{B(D \to \text{all})} \quad . \tag{11}$$

In addition to $K + n\pi$, "all" will include $K\eta + n\pi$, semi-leptonic decays, and Cabbibo suppressed decays. In Table IV we list the prediction times $f_{Kn\pi}$ divided by the measurement. We would expect $f_{Kn\pi}$ to have a value of

around 0.6 to 0.7, if, as we will soon see, the semileptonic branching fractions are of the order of 0.2 for the sum of electronic and muonic modes. The value of $f_{Kn\pi}$ seems smaller than this if deduced from modes with all charged particles, but, with sizeable errors, larger than this if deduced from the $K^-\pi^+\pi^o$ mode.

E. Charm Production at 4.028 and 4.414 GeV

With the absolute branching fractions from Table III we are now in a position to calculate the amount of charm production at two of the prominent peaks in the 4 GeV region.

The inputs are

a) $\sigma \cdot B$ from Table II, and

b) B from Table III.

There are no additional assumptions to those already used in constructing Table III.

We define $R_D = \sigma_D / 2\sigma_{\mu\mu}$. The factor of 2 in the denominator takes into account the fact that charmed particles are produced in pairs, so that R_D can be directly compared to the total hadronic R. In particular, we compare it to

$$R_{new} \equiv R - R_{old} - R_\tau \qquad (12)$$

where R is taken from measurements of the total hadronic cross section,[6,17] R_{old} (2.4) is taken from measurements of the total hadronic cross section below charm threshold,[4] and R is the theoretical expression for the production of a 1.9 GeV/c^2 mass lepton.

$$R_\tau = \tfrac{1}{2}\beta(3 - \beta^2) \quad . \qquad (13)$$

If D's and τ's are the only new particles being produced then R_{new} should equal R_D. If the production of F's, charmed baryons, or even other new

particles are sizable, then R_{new} will be larger than R_D.

The results are given in Table V. R_{D^o} is calculated from all observed D^o modes and also from just the better-measured $K^{\mp}\pi^{\pm}$ mode. At 4.028 GeV these two measurements are consistent and R_{new} is consistent with being equal to R_D. At 4.414 GeV the two measurements differ somewhat, but nevertheless it is clear that whatever else may be happening at 4.414 GeV, most of the excess cross section is going into D production. Note that the fraction of charged D production at 4.028 GeV is significantly smaller than that at 3.774 GeV where we have assumed $R_{D^\pm}/R_D = 0.44 \pm 0.03$. In the near future one should be able to combine this result with inclusive lepton production at 4.028 and 3.774 GeV to calculate the ratio of D^+ to D^o semileptonic branching fractions. Since semileptonic decays are $I = 0$ transitions, this rate is the inverse of the ratio of D^+ to D^o lifetimes.[24]

IV. Branching Fractions into Semi-leptonic Decay Modes

The general technique which has been used to measure the semi-electronic branching fraction of D mesons is to count the number of electrons in events in which three or more charged particles are detected, correct for backgrounds and losses, and divide by the total cross section for charm production. There are several problems inherent in this approach:

a) It is necessary to subtract garden variety backgrounds such as γ conversions, Dalitz pairs, and ψ and ψ' decays. This is straightforward but these backgrounds can become large at low electron momentum and limit the statistical accuracy in this region.

b) Around 15% of τ decays involving an electron are expected to occur in events with more than two charged particles, and these decays must be subtracted. This is not a serious problem in practice since this τ contribution is relatively small and relatively well known.[25]

c) Some D decays involving an electron will not be counted because they occur in events with only two charged particles. This correction is relatively small, but somewhat model dependent.

d) Each experiment has some momentum below which the cannot detect electrons. Accordingly, a correction must be made for that part of the electron spectrum which is below this threshold. This correction is also model dependent, but fortunately this model dependence partially cancels that of the correction for two-prong D decays.[26]

e) One must determine the total cross section for charm production in order to divide by it. Curiously, at present it appears that discrepancies between different experiments are due more to differences in the total cross sections they measure than to the number of electrons they count.

f) Finally, what is measured is a natural average of charm particle semi-leptonic decays. As we have seen, at 3.772 GeV there are roughly equal numbers of neutral and charged D's, while at 4.028 GeV, there are probably slightly over twice as many neutral D's as charged D's. At higher energies F's and charmed baryons will contribute to the average. As we have already mentioned, in the future we will be able to use these differences to unfold the various particles decays. For the present, however, they only contribute some additional uncertainty to the measurements. In order to concentrate on the D meson branching ratios and to reduce as much as possible the model dependence of the results, we will study only the measurements at the lowest possible c.m. energies.

Three experiments have now measured the average D meson semi-electronic branching fractions. Table VI lists these epxeriments, the electron detection technique, the solid angle, the lowest c.m. energy, and the average semi-electronic branching fraction measured at that energy.[26-29] The DELCO experiment at SPEAR,

is shown in Fig. 11, is exceptional in having excellent electron detection and an order of magnitude more solid angle than the other two experiments. Its statistical power is shown in Fig. 12 where the ψ'' line shape is clearly seen in the cross section for electron production as a function of c.m. energy.

The three experiments are in good agreement given the sizeable statistical and systematic errors. The world average of about 9% is about a factor of two smaller than the 20% which would be expected from naive quark and lepton counting.

Each of the three experiments has measured the electron momentum spectrum, shown in Figs. 13-15. All of the spectra agree with the relatively soft spectra expected from $Ke\nu$ and $K^*e\nu$ decay modes, and all of the experiments can obtain good fits to their spectra if they include sizeable fractions of these two modes. None of the experiments has had the sensitivity to study the V,A structure of the $K^*e\nu$ decay mode. This remains probably the single most interesting outstanding question in the study of D meson decays.

V. Tagged Events

With the discovery of the ψ'', it becomes possible for the first time to "tag" charmed particle decays. For example, if we detect a D^o decay into $K^-\pi^+$ in a ψ'' decay, then we are also looking, essentially without bias, at a $\overline{D^o}$ decay where the $\overline{D^o}$ has a momentum of 300 MeV/c in a known direction. In this section, we will give some examples, based on a preliminary analysis, of the type of studies which are possible with tagged events. In the future this technique will probably become the prime method of studying D mesons.

A. Decays With All Charged Particles

In section III.C. we determined absolute D branching fractions by employing some very reasonable assumptions about the nature of ψ''. We can now check these assumptions by using tagged events to measure D branching fractions.

We use the five decay modes shown in Fig. 2 as the tagging decays and

look for events in which all or all but one of the decay products of the other D are detected. There are 194 tagging D^o decays and 82 tagging D^- decays.

We find eight cases of $K^-\pi^+$ or $K^-\pi^+\pi^-\pi^+$ decay opposite the tagging decays. These eight cases come from six events because in two cases both halves of the event tag each other, and such events must be counted twice. Correcting for detection and triggering efficiencies, these events give

$$B(D^o \to K^-\pi^+ \text{ or } K^-\pi^+\pi^-\pi^+) = (6.2 \pm 2.7)\% \qquad (14)$$

which is consistent with the value of $(5.4 \pm 1.5)\%$ from Table III.

There are two cases of a $K^-\pi^+\pi^-$ decay opposite a tagging D^- decay. each from a separate event. These two events give

$$B(D^+ \to K^-\pi^+\pi^+) = (3.4 \pm 2.4)\% \quad , \qquad (15)$$

which is in good agreement with the value of $(3.9 \pm 1.0)\%$ from Table III.

We can now turn these results around and use them to calculate ψ'' branching fractions without the aid of any assumptions.

The inputs are

a) $\sigma \cdot B$ for D decays at the ψ'' (Table II),

b) B for D decays from the tagged events (Eqs. 14 and 15), and

c) ψ'' total cross section measurements.[4,17]

The results are given in Table VII along with the values which were assumed in section III.C. The agreement is excellent, but given the enormous errors, clearly fortuitous.

B. Decays With One Missing Neutral

We can also look for events with a charged kaon, another charged particle, and a missing, near zero-mass, neutral particle opposite a tagging D^o decay. These decays could be $D^o \to K^-\pi^+\pi^o$, $D^o \to K^-e^+\nu$, or $D^o \to K^-\mu^+\nu$ modes, which we shall designate as $D_{\pi 3}$, D_{e3}, and $D_{\mu 3}$ for short. There are

ten cases of these events, which leads to

$$B(D_{\pi 3}) + B(D_{e3}) + B(D_{\mu 3}) = (11.7 \pm 4.1)\% \quad . \tag{16}$$

Unfortunately it is quite difficult to distinguish between $D_{\pi 3}$, D_{e3}, and $D_{\mu 3}$ decays in the magnetic detector because

a) the leptons often have low momentum and are not discriminated from pions, and

b) low energy π^o's are difficulty to detect.

However, we can obtain some information on D_{e3} decays by subtracting the measured branching fraction for $D_{\pi 3}$ decays, $(12 \pm 6)\%$[19] and setting $B(D_{e3}) = B(D_{\mu 3})$. This gives

$$B(D^o \to K^- e^+ \nu) < 3.6\% \text{ at } 1\sigma \text{ c.l.} \tag{17}$$

Dividing by the world average given in Table VI,

$$\frac{B(D^o \to K^- e^+ \nu)}{B(D^o \to e^+ + \text{anything})} < 39\% \text{ at } 1\sigma \text{ c.l.} \tag{18}$$

By fitting $Ke\nu$ and $K^*e\nu$ spectra to their measured electron momentum spectrum (see Fig. 13), the DASP group obtained $(35 \pm 30)\%$ for the ratio given in Eq. 18.[27]

C. Charged Multiplicity in D Decays

To determine the charged multiplicities in D decays, we count the charged particles opposite a tagging decay and use a Monte Carlo calculation of efficiencies to unfold the true distributions from the observed distributions. In this preliminary analysis we have used only the $K^+\pi^-$ and $K^+\pi^-\pi^-$ modes as tagging decays. Backgrounds, which are typically about 10% have been explicitly subtracted from the data. No attempt has been made to identify neutral kaons so that a K_s decaying to two charged pions will count as two charged particles.

The raw data are displayed in the top portion of Fig. 16 and the unfolded data are displayed in the bottom portion. D^o's decay primarily to two charged particles, while D^+'s decay to roughly equal numbers of one and three charged particles. The mean charged multiplcities are

$$\langle n_c \rangle_{D^o} = 2.3 \pm 0.2 \tag{19}$$

$$\langle n_c \rangle_{D^+} = 2.3 \pm 0.3 \quad . \tag{20}$$

The statistical model assumed somewhat higher charged multiplicities, typically about 2.7.[23]

D. Two-prong $D\bar{D}$ Decays

Events in which only two charged particles are produced are of special interest experimentally because

a) there is background in two-prong events from QED processes,

b) they have a much lower detection efficiency in the magnetic detector and most other detectors, and

c) $\tau^+\tau^-$ decays occur primarily in two-prong events.

We can calculate the fraction of $D\bar{D}$ decays that go into two charged particles directly from the data in Fig. 16:

$$D^o\bar{D^o} : 2f_o f_2 = (11 \pm 7)\% \tag{21}$$

$$D^+D^- : f_1^2 = (17 \pm 8)\% \quad . \tag{22}$$

Here f_n represents the fraction of decays to n charged particles. The fractions of two charged particle events given by Eqs. 21 and 22 are not vastly different from the overall fraction of two prong events. We thus expect to see the same type of variation with energy in the two prong cross section as in the mutliprong cross section.

Semileptonic decays of D's and leptonic decays of τ's are often separated experimentally by multiplicity: the D's are presumed to decay primarily into events with four or more charged particles while τ's are presumed to decay primarily into events with two charged particles. It is thus important to measure the extent to which semileptonic D decays can occur in two-charged-prong events. We do not presently have enough information to determine this but we can set upper limits by assuming that semileptonic decays always occur in the lowest possible charged multiplicities.

For $D^o\overline{D^o}$ decays the lowest charged multiplicity is clearly two, therefore

$$D^o\overline{D^o} \text{ 2-prong lepton fraction} < f_o$$
$$< 13\% \text{ at } 1\sigma \text{ c.l.} \qquad (23)$$

For D^+D^- decays one might expect that the upper limit is just f_1. However we can obtain a better limit if we assume that Cabbibo suppressed decays are unimportant. Then the simplest semileptonic decay is $D^+ \to K^o\ell^+\pi$. The $\overline{K^o}$ looks like zero prongs two-thirds of the time and like two prongs one-third of the time. Therefore

$$D^+D^- \text{ 2-prong lepton fraction} < 0.66\ f_1$$
$$< 34\% \text{ at } 1\sigma \text{ c.l.} \qquad (24)$$

VI. Spins and Parities

If the D meson family is similar to other mesons, then we would expect the lowest lying state to be a pseudoscalar ($J^P = 0^-$) and the second lowest lying state to be a vector particle ($J^P = 1^-$). Although a combination of the experimental data and our theoretical prejudice that low lying states should have low spins strongly favor this choice, it is worthwhile to state precisely what we have determined about D meson spins and parities from experimental measurements alone:

a) The absolute D parity cannot be measured. This is simply because in reactions in which charm is not conserved, parity is also not conserved.[30] We are thus free to define the D parity,

$$P_D = -1 \quad . \tag{25}$$

If the D is a bound s-wave state of two quarks, then this definition sets the parity of the charmed quark equal to the parity of the other quarks,

b) If either the D or D* has spin 0, then from the observation of $D^* \to D\pi$,[13]

$$P_{D^*} = (-1)^{J_D + J_{D^*}} \quad . \tag{26}$$

c) Both the D and D* cannot have spin 0. If they did then from Eq. (26), the D* would be a scalar particle. But the reaction

$$e^+e^- \to D\bar{D}^* \tag{27}$$

has clearly been observed[12] and e^+e^- annihilation through a single virtual photon cannot couple to a scalar plus a pseudoscalar by parity conservation.

d) The next simplest hypothesis is that the sum of the absolute value of the two spins is one. There are two possibilities:

$$J_D^P = 0^- \text{ and } J_{D^*}^P = 1^- \tag{28a}$$

or

$$J_D^P = 1^- \text{ and } J_{D^*}^P = 0^- \quad . \tag{28b}$$

Three independent measurements strongly favor the former of these possibilities:

i) The angular distributions for

$$e^+e^- \to D\bar{D}^* \tag{29}$$
$$\hookrightarrow K\pi$$

are of the form

$$P(\Theta,\theta) \propto 1 + \cos^2\Theta \tag{30}$$

for hypothesis (28a) and of the form

$$P(\Theta,\theta) \propto \sin^2\theta \ (1 + \cos^2\Theta) \qquad (31a)$$

for hypothesis (28b), where Θ is the angle between the DD* production direction and the incident beams, and θ is the angle between the Kπ decay direction and the D momentum in the D center of mass. It is clear from Eqs. (30) and (31a) that one should look at the θ dependence. This is done in Fig. 17b, for 4.028 GeV data.[31] Equation (30) has a confidence level of 51% while Eq. (31a) has a confidence level of 0.6%.

Another way of studying these same data with different systematic errors has also been used. First Eq. (31a) is expanded to include the dependence on the azimuthal angle between $D\bar{D}^*$ production plane and the D decay plane, :

$$P(\Theta, \theta, \phi) \propto \sin^2\theta \ (\cos^2\phi + \cos^2\Theta\sin^2\phi). \qquad (31b)$$

Then the events are divided into two groups depending on whether the right side of Eq. (31b) is greater or less than 0.32, and a Kπ invariant mass spectrum is constructed for each set of events. The number of events in each group is extracted by fitting the spectra, as shown in Fig. 18. For hypothesis (28a) there should be roughly equal numbers of events in the two groups, while for hypothesis (28b) there should be more than twice as many events in Fig. 18b as in Fig. 18a. The data are consistent with hypothesis (28a) with a confidence level of nearly 100% and inconsistent with hypothesis (28b) with a confidence level of only 0.35%.

ii) Additional evidence favoring hypothesis (28a) over (28b) comes from measurements of the production angle for $D^*\bar{D}^*$ and $D\bar{D}$ final states. Here the dependence on Θ must be

$$P(\Theta) \propto 1 + \alpha\cos^2\Theta, \qquad (32)$$

where $|\alpha| < 1$ in general and $\alpha = -1$ for spin 0. For $D^*\bar{D}^*$ production at 4.028 GeV[31] the θ distribution is shown in Fig. 17c and

$$\alpha_{D^*_0} = -0.30 \pm 0.33 \ . \qquad (33)$$

This represents a 2% confidence level for the D* spin to be zero.

In contrast the Θ distributions for $D\bar{D}$ production at 3.774 GeV[10] is shown in Fig. 19. The fits to Eq. (32) give

$$\alpha_{D^o} = -1.00 \pm 0.09 \qquad (34a)$$

and

$$\alpha_{D^+} = -1.04 \pm 0.10 \quad ,$$

in complete agreement a spin zero assignment for the D. While these data do not prove the D spin is zero, it seems unlikely that a particle of higher spin would give $\alpha \approx -1$ by accident.

Thus, to conclude, if $|J_D| + |J_{D^*}| < 2$, the data allow only the assignment given in (28a). In addition, there is circumstantial evidence that independent of the D* spin, the D has spin zero.

VII. $D^o - \overline{D^o}$ Mixing

In principle, the D^o and $\overline{D^o}$ could mix in much the same way as the K^o and $\overline{K^o}$ mix to form the K_s and K_L. If the GIM mechanism works for charm then the time scale for mixing should be long compared to the D^o lifetime and there should be a negligible amount of mixing, around 0.2%. On the other hand, if there is even a small charm-changing neutral current, then the time scale for mixing should be small compared to the D^o lifetime and there should be complete D^o-$\overline{D^o}$ mixing -- that is, D^o's should decay equally to states of positive and negative strangeness.[32]

Two independent measurements find no evidence for D^o-$\overline{D^o}$ mixing in agreement with the standard model. One technique has been to find $D^o \to K^- \pi^+$ decays in the 4 GeV region in which the kaon is well identified by time of flight and search for additional well identified charged kaons.[12] Of 77 events, in 62 the kaons appear to have opposite charge and in 15 events they appear to have the same charge. However 16 events with kaons of apparently the same charge are expected in the absence of mixing from π-K misidentifications. Thus, there is no

evidence for mixing and the fraction of events containing a D^o which exhibit strangeness violation is less than 18% at the 90% confidence level.

The second technique has been to study $D^{*+} \to D^o\pi^+$ decays. In these decays the sign of the cascade pion tags the charm content of the D^o. One can then measure the sign of the strangeness, that is, the fraction of the time the D^o decays to $K^+\pi^-$ instead of $K^-\pi^+$. A glance at Fig. 5 shows that $D^{*+} \to (K^-\pi^+)\pi^+$ decays (Fig. 5a) are much more common than $D^{*+} \to (K^+\pi^-)\pi^-$ decays. To obtain a more sensitive measure, we can eliminate events in which the kaons are not well identified. There remain 26 events in the peak in Fig. 5a and only three events in the same region in Fig. 5b, two of which are expected from backgrounds and misidentifications. Thus again, there is no evidence for D^o-$\overline{D^o}$ mixing and the fraction of D^o's which decay to states of positive strangeness is less than 16% at the 90% confidence level.

VIII. F^+ Mesons

Compared to the detailed information which has been compiled on D mesons, we have only a few hints concerning the F^+ mesons, $c\bar{s}$ bound states. The DASP group has reported four events at 4.4 GeV which can be fit to the hypothesis of either an $F\bar{F}^*$ or $F^*\bar{F}^*$ final state.[33] In these events they observe the decay $F^* \to F\gamma$. The mass of the F is determined to be 2039 ± 60 MeV/c^2. The large uncertainty in mass comes partially from the ambiguity of whether the final state was $F\bar{F}^*$ or $F^*\bar{F}^*$.

The second hint comes from SPEAR magnetic detector data at 4.16 GeV. There is a peak in the invariant mass spectrum for the sum of $K^+K^-\pi^\pm$, $K_sK^\pm$, and $K^+K^-\pi^+\pi^-\pi^\pm$ final states fit to be hypothesis of $F\bar{F}$ production.[34] The mass is accurately determined (by the same technique which was used for D mesons) to be 2039.5 ± 1.0 MeV/c^2 The significance of this result is still being investigated.

Either or both of these results may turn out to be correct, but in both cases the level of significance is certainly less than that of the original data

which showed the existence of D mesons.[2,3] Second generation detectors such as the Mark II at SPEAR should be able to easily confirm or deny these results in the near future.

IX. Charmed Baryons

Our experimental information on charmed baryons is also somewhat meager. There have been two reports of observation of the Λ_c^+, the isosinglet cud bound state. The first is a single neutrino event in the Brookhaven 7-ft bubble chamber of the form[35]

$$\nu p \rightarrow \mu^- \Lambda \pi^+ \pi^+ \pi^+ \pi^- \quad . \tag{35}$$

This event violates the $\Delta S = \Delta Q$ rule and thus is likely to have a charm baryon decay in the final state. The mass of one $\Lambda\pi^+\pi^+\pi^-$ combination is 2.26 GeV/c^2.

The second report is of a peak in the inclusive $\bar{\Lambda}\pi^-\pi^-\pi^+$ mass spectrum at 2.26 GeV/c^2 from high energy photoproduction at Fermilab.[36] Although the authors do not give a production cross section corresponding to this peak, it is clear that it is sizeable and that it implies the exciting possibility of a rather large photoproduction cross section for charmed particles, perhaps close to 1 μb. An improved version of this experiment is currently running at Fermilab and results should be available soon.

No peaks in invariant mass spectra corresponding to any charmed baryons have been seen in e^+e^- annihilation. Upper limits have been set which are about an order of magnitude lower than typical $\sigma \cdot B$ measurements for D meson production at the same energies.[34] The only positive indication in e^+e^- annihilation is a sharp rise in inclusive baryon production from around 4.4 GeV to 5.0 GeV,[37] the threshold region for charmed baryon production. The proton and Λ data are shown in Figs. 20a and 20b. The statistical accuracy of the Λ data is too low to establish the precise region in which the rise occurs. However, the most significant feature is that the Λ cross sections are consistent with being between 10 and 15% of the proton cross sections at all energies.

This low value tends to indicate that charmed baryons may preferentially decay into final states containing protons and kaons rather than states containing strange baryons.

References and Footnotes

1. In addition to charmed particle spectroscopy, the topics of the charmonium spectroscopy and the τ lepton were covered in the oral version of these lectures. These latter two topics have been omitted from the written version because they are adequately reviewed elsewhere. For a discussion of both these topics see G.J. Feldman and M.L. Perl, Phys. Rep. 33C, 285 (1977), also issued as SLAC report SLAC-PUB-1972 (1977). A few more recent results can be found in G.J. Feldman in the Proceedings of the V International Conference on Experimental Meson Spectroscopy, Northesastern University, Boston, Mass., April 29-30, 1977, also issued as SLAC report number SLAC-PUB-1977 (1977) and M.L. Perl in the Proceedings of the 1977 International Symposium on Lepton and Photon Interactions at High Energies, Hamburg, Germany, August 25-31, 1977, also issued as SLAC report SLAC-PUB-2022 (1977). The lecture notes presented here are based in part on G.J. Feldman in the Proceedings of SLAC Summer Institute on Particle Physics, July 11-22, 1977, Stanford, Calif., also issued as SLAC report number SLAC-PUB-2000 (1977).

2. G. Goldhaber et al., Phys. Rev. Lett. 37, 255(1976).

3. I. Peruzzi et al., Phys. Rev. Lett. 37, 569(1976).

4. P.A. Rapidis et al., Phys. Rev. Lett. 39, 526(1977).

5. W. Bacino et al., SLAC report number SLAC-PUB-2030 (1977).

6. J. Siegrist et al., Phys. Rev. Lett. 36, 700(1976).

7. P.B. Wilson et al., SLAC report number SLAC-PUB-1894 (1977).

8. In our error analysis, we have assigned the error due to the long-term drift in E_b determination to be 0.5 MeV. This is probably conservative.

9. V. Lüth et al., Phys. Lett. 70B, 120(1977).

10. I. Peruzzi et al., Phys. Rev. Lett. 39, 1301(1977).

11. D.B. Lichtenberg, Phys. Rev. D12, 3760(1975); A. De Rujula, H. Georgi, and S.L. Glashow, Phys. Rev. Lett. 37, 398(1976); K. Lane and S. Weinberg, Phys. Rev. Lett. 37, 717(1976); S. Ono, Phys. Rev. Lett. 37, 655(1976); W. Celmaster, Phys. Rev. Lett. 37, 1042(1976); H. Fritzsch, Phys. Lett. 63B, 419(1976); J. Dabaul and M. Krammer, Phys. Lett. 64B, 341(1976); N.G. Deshande et al., Phys. Rev. Lett. 37. 1305(1976); J.S. Guillen, Lett. al Nuovo Cimento 18, 218(1977); D.H. Boal and A.C.D. Wright, Phys. Rev. D16, 1505(1977); L.H. Chan, Lousiana State University report (1976); D.C. Peasleee, Phys. Rev. D15, 3495(1977); and N.F. Nasrallah and K. Schilcher, Universitat Mainz report NZ-TH 76/15 (1976).

12. G. Goldhaber et al., Phys. Lett. 69B, 503(1977).

13. G.J. Feldman et al., Phys. Rev. Lett. 38, 1313(1977).

14. The value is from the "normal fit" of Ref. 12. The "isospin constrained

fit" give an erroneous value for $B(D^{o*} \to D^o\gamma)$ because the D^+ mass was fit to be 1873 MeV/c^2. This forbade the decay $D^{*+} \to D^+\pi^o$ and forced all $D^{*+} \to D^+$ decays into the mode $D^{*+} \to D^+\gamma$, which in turn forced too high a value of $B(D^{o*} \to D^o\gamma)$ through the constraint conditions.

15. See F.J. Gilman in the Proceedings of the SLAC Summer Institute on Particle Physics, July 11-22, 1977, Stanford, Calif. for a discussion of the validity of these models for ordinary quarks.

16. M. Piccolo et al., Phys. Lett. 70B, 260(1977).

17. The values of Refs. 4, 6, and 16 have been reduced by 7.5% to account for a revised calculation of the external radiative correction for Bhabha scattering. See footnote 11 of Ref. 10.

18. A. Barbaro-Galtieri et al., Phys. Rev. Lett. 39, 1058(1977).

19. D.L. Scharre et al., SLAC report number SLAC-PUB-2019 (1977).

20. J.D. Jackson, Nuovo Cimento 34, 1645(1964); A. Barbaro-Galtieri in Advance in Particle Physics, edited by R.L. Cool and R.L. Marshak (Wiley, new York), Vol. II, 1968.

21. In Ref. 4, acceptable fits for the ψ'' line shape were obtained for all values of r greater than one fm.

22. G. Altarelli, N. Cabibbo, L. Maiani, Nucl. Phys. B88, 285(1975); R.L. Kingsley, S.B. Treiman, F. Wilczek, and A. Zee, Phys. Rev. D11, 1919(1975); M.B. Einhorn and C. Quigg, Phys. Rev. D12, 2015(1975).

23. J.L. Rosner, Invited talk at Orbis Scientiae, Jan. 17-21, 1977, Coral Gables, Fla., (Institute for Advanced Study report COO-2220-120).

24. A. Pais and S.B. Treiman, Phys. Rev. D15, 2529(1977).

25. See references given in Footnote 1.

26. J.M. Feller et al., SLAC report number SLAC-PUB-2028(1977).

27. R. Brandelik et al., Phys. Lett. 70B, 387(1977).

28. J. Krikby in the Proceedings of the 1977 International Symposiun on Lepton and Photon Interactions at High Energies, Hamburg, Germany, August 25-31, 1977, also issued as SLAC report number SLAC-PUB-2040 (1977).

29. The experimental results given here are the best known values as of the writing of this report and thus differ slightly from those given in the oral version.

30. J.E. Wiss et al., Phys. Rev. Lett. 37, 1531(1976).

31. H.K. Nguyen et al., Phys. Rev. Lett. 39, 262(1977).

32. See Ref. 13 for an extensive list of references on this topic.

33. R. Brandelik et al., Phys. Lett. 70B, 132(1977).

34. D. Lüke, Proceedings of the 1977 Meeting of the Division of Particles and Fields of the American Physical Society, Argonne National Laboratory, Argonne, Ill., Oct. 6-8, 1977.

35. E.G. Cazzoli et al., Phys. Rev. Lett. 34, 1125(1975).

36. B. Knapp et al., Phys. Rev. Lett. 37, 882(1976).

37. M. Piccolo et al., Phys. Rev. Lett. 39, 1503 (1977).

TABLE I

D^* branching fractions and widths. See the text for a discussion of the input data and the assumptions which were used.

	D^{*o}	D^{*+} $\frac{m_u}{m_c} = \frac{m_\rho}{m_\psi}$	D^{*+} $\frac{m_u}{m_c} = 0$
$B(D^* \to D\pi^{\pm})$	0	0.68 ± 0.08	0.63 ± 0.09
$B(D^* \to D\pi^o)$	0.55 ± 0.15	0.30 ± 0.08	0.27 ± 0.07
$B(D^* \to D\gamma)$	0.45 ± 0.15	0.02 ± 0.01	0.10 ± 0.05
$\Gamma(D^{*o})/\Gamma(D^{*+})$	---	1.0 ± 0.3	0.9 ± 0.3

TABLE II

$\sigma \cdot B$ in nb for various D decay modes at three values of $E_{c.m.}$ See footnote 17.

		$E_{c.m.}$ (GeV)		
		3.774	4.028	4.414
D^o	$K^{\mp}\pi^{\pm}$	0.25 ± 0.05	0.53 ± 0.10	0.28 ± 0.08
	$\bar{K}^o\pi^+\pi^-$ + c.c	0.46 ± 0.12	1.01 ± 0.28	0.85 ± 0.32
	$K^{\mp}\pi^{\pm}\pi^+\pi^-$	0.36 ± 0.10	0.77 ± 0.25	0.85 ± 0.36
	$\pi^+\pi^-$	---	< 0.04	---
	K^+K^-	---	< 0.04	---
	Total D^o observed modes	1.07 ± 0.21	2.31 ± 0.39	1.97 ± 0.49
D^+	$\bar{K}^o\pi^+$ + c.c	0.14 ± 0.05	< 0.17	---
	$K^{\mp}\pi^{\pm}\pi^{\pm}$	0.36 ± 0.05	0.37 ± 0.09	0.31 ± 0.11
	$\pi^{\mp}\pi^+\pi^-$	---	< 0.03	---

TABLE III

D branching fractions for hadronic decay modes. See the text for a discussion of the input data and the assumption which were used.

Mode		Branching fraction (%)
D^o	$K^-\pi^+$	2.2 ± 0.6
	$\overline{K^o}\pi^+\pi^-$	4.0 ± 1.3
	$K^-\pi^+\pi^o$	12 ± 6
	$K^-\pi^+\pi^-\pi^+$	3.2 ± 1.1
D^+	$\overline{K^o}\pi^+$	1.5 ± 0.6
	$K^-\pi^+\pi^+$	3.9 ± 1.0

TABLE IV

Comparison of the D branching fractions from Table III with the statistical model of Ref. 23. See text for the definition of $f_{Kn\pi}$.

Mode		prediction/measurement
D^o	$K^-\pi^+$	$(2.7 \pm 0.7)\ f_{Kn\pi}$
	$\overline{K^o}\pi^+\pi^-$	$(3.0 \pm 1.0)\ f_{Kn\pi}$
	$K^-\pi^+\pi^o$	$(0.8 \pm 0.4)\ f_{Kn\pi}$
	$K^-\pi^+\pi^-\pi^+$	$(2.2 \pm 0.8)\ f_{Kn\pi}$
D^+	$\overline{K^o}\pi^+$	$(8.7 \pm 3.5)\ f_{Kn\pi}$
	$K^-\pi^+\pi^+$	$(2.6 \pm 0.7)\ f_{Kn\pi}$

TABLE V

Charm production at 4.028 and 4.414 GeV. See text for definitions and a discussion of the input data and assumptions which were used.

	4.028 GeV		4.414 GeV	
	all D^o modes	$K^{\mp}\pi^{\pm}$ only	all D^o modes	$K^{\mp}\pi^{\pm}$ only
R_{D^o}	2.3 ± 0.6	2.2 ± 0.8	2.3 ± 0.8	1.4 ± 0.6
$R_{D^{\pm}}$	0.9 ± 0.4	0.9 ± 0.4	0.9 ± 0.4	0.9 ± 0.4
R_D	3.2 ± 0.7	3.1 ± 0.9	3.2 ± 0.9	2.3 ± 0.7
R_{new}	3.1 ± 1.0	3.1 ± 1.0	2.5 ± 1.0	2.5 ± 1.0
$R_{D^{\pm}}/R_D$	0.28 ± 0.09	0.29 ± 0.10	0.38 ± 0.11	0.39 ± 0.13

TABLE VI

Semi-electronic D meson branching fractions.

Experiment	technique	Ω	lowest $E_{c.m.}$	$\langle B_e \rangle$ (%)
DASP[27]	Cerenkov and shower counters	7%	3.99 to 4.08	10 ± 3
LGW[26]	Lead glass	6%	3.774	7.2 ± 2.8
DELCO[28]	Cerenkov and shower counters	60%	3.774	11 ± 3
		World average		9.3 ± 1.7

TABLE VII

ψ'' branching fractions in per cent. See the text for a discussion of the input data

	B measured	B (assumed in Sec. III.C.)
$\psi'' \to D^{\circ}\overline{D^{\circ}}$	49 ± 25	56 ± 3
$\psi'' \to D^{+}D^{-}$	50 ± 38	44 ± 3
$\psi'' \to D\bar{D}$	99 ± 48	100

FIGURE CAPTIONS

1. R in the threshold region for charmed meson production.

2. Invariant mass spectra for various D decay modes at the ψ''.

3. Invariant mass spectra for the sum of all observed (a) D^+ and (b) D^o decay modes decaying into all charged particles.

4. D momentum spectra at 4.028 GeV for (b) $D^o \to K^{\mp}\pi^{\pm}$ and (c) $D^{\pm} \to K^{\mp}\pi^{\pm}\pi^{\pm}$. The solid curves represent an isospin constrained fit to the data. (a) shows the various contributions to the fit in (b). A, B, and C are contributions from $D^*\bar{D}^*$ production with A: $D^{*+} \to D^o\pi^+$, B: $D^{*o} \to D^o\pi^o$ and C: $D^{*o} \to D^o\gamma$. D, E, F, and G are contributions from $D^*\bar{D}$ and $D\bar{D}^*$ production with D: $D^{*+} \to D^o\pi^+$, E: $D^{*o} \to D^o\pi^o$, F: direct D^o, and G: $D^{*o} \to D^o\gamma$. H is the contribution from $D^o\bar{D}^o$ production.

5. $D\pi$ - D mass difference spectra for (a) $D^o\pi^+$ and $\bar{D}^o\pi^-$ combinations and (b) $\bar{D}^o\pi^+$ and $D^o\pi^-$ combinations.

6. Q values for $D^* \to D$ transitions.

7. Invariant mass spectra for various D decay modes at 4.028 and 4.414 GeV.

8. The SPEAR magnetic detector as seen looking along the incident beams. The proportional chambers around the beam pipe and the trigger counters are not shown. The LGW is shown on the left of the detector.

9. (A) Two photon invariant mass distribution for photon pairs detected in the LGW. A photon energy cutoff of 150 MeV is required for events in the shaded region. (b) π^o acceptance in the LGW as a function of π^o momentum.

10. $K^{\mp}\pi^{\pm}\pi^o$ invariant mass distribution for constarined events.

11. The DELCO apparatus at SPEAR as seen (a) perpendicular to the incident beams and (b) along the incident beams.

12. R_e, the ratio of the cross section for inclusive electrons in multi-particle events to the theoretical cross section for μ pair production, in the vicinity of the ψ''.

13. The momentum spectrum of inclusive electrons in multi-particle events in the $E_{c.m.}$ range 3.99 to 4.08 GeV as measured by the DASP collaboration. Curves show theoretical spectra expected for $K^*e\nu$ and $Ke\nu$ D decay modes.

14. The momentum spectrum of inclusive electrons in multi-particle decays of the ψ'' as measured by the LGW experiment on the SPEAR magnetic detector. Curves show theoretical spectra expected for $K^*e\nu$, $Ke\nu$, and $\pi e\nu$ D decay modes.

15. The momentum spectrum of inclusive electrons in multi-particle decays of the ψ'' as measured by the DELCO experiment. The solid and dashed curves show theoretical spectra expected for $K^*e\nu$ and $Ke\nu$ D decay modes. The dot-dashed curve indicates the estimated background remaining in the data.

16. Observed and true (unfolded) charged multiplicities for D decays.

17. (a) Θ distribution of D^{o} in reaction (27). Solid curve corresponds to hypothesis (28a) and dashed curve corresponds to hypothesis (28b). The dot-dashed curve corresponds to spinless D's and D*'s. (b) θ distribution in reaction (27). Curves as in part (a). (c) Θ distribution for D^{o}'s from $D^{*}\overline{D^{*}}$ production. Curve is a fit to Eq. (32).

18. Invariant mass spectra of $K^{\mp}\pi^{\pm}$ decay modes in reaction (27) for (a) low and (b) high values of the right side of Eq. (31b).

19. θ distributions for (a) $K^{\mp}\pi^{\pm}$ and (b) $K^{\mp}\pi^{\pm}\pi^{\pm}$ decay modes from $D\bar{D}$ production. The curves represent Eq. (32) with $\alpha = -1$.

20. The ratios of cross sections for (a) inclusive p plus $\bar{p}$ production, (b) inclusive Λ plus $\bar{\Lambda}$ production, and (c) hadron production to the theoretical cross section for μ pair production.

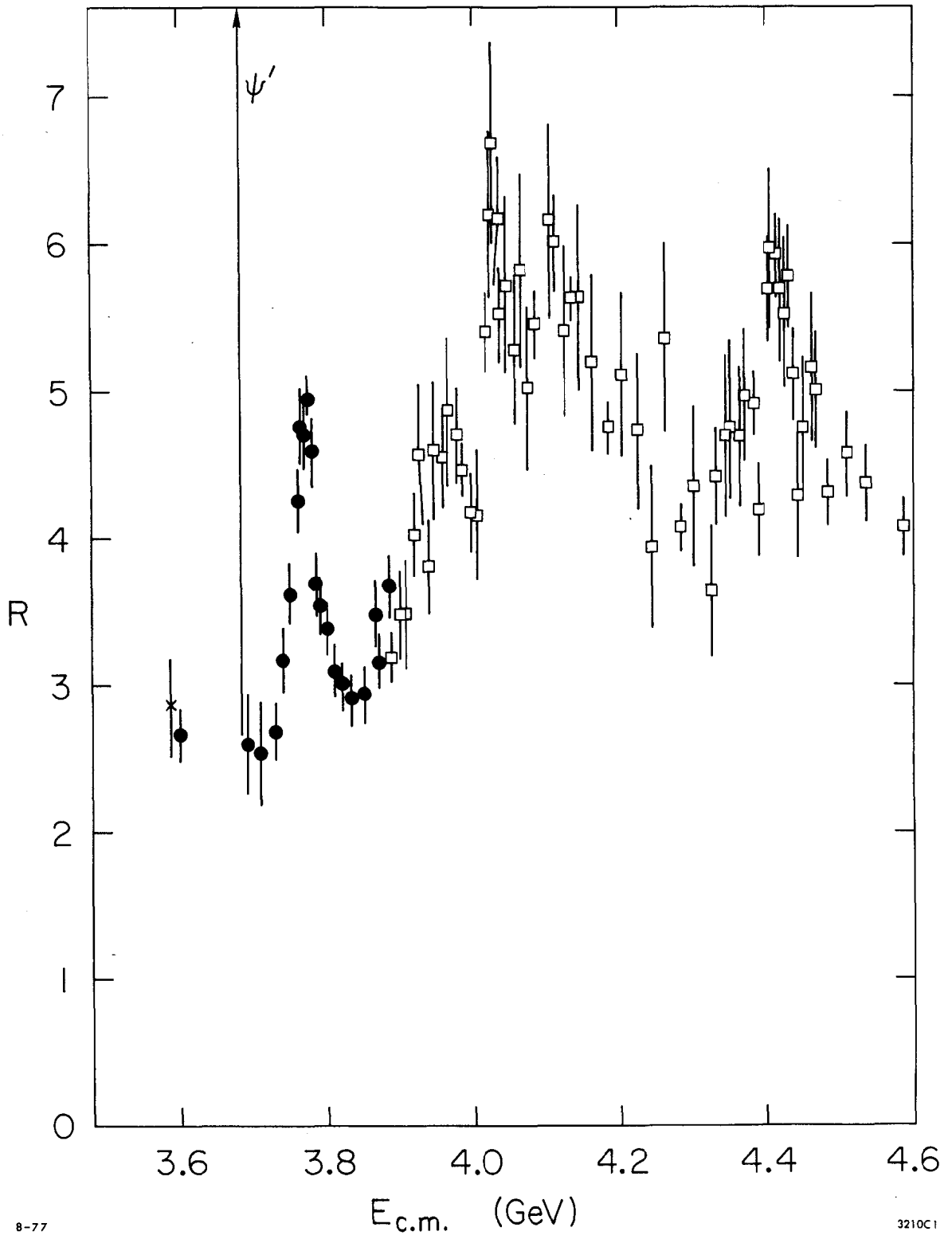

Fig. 1

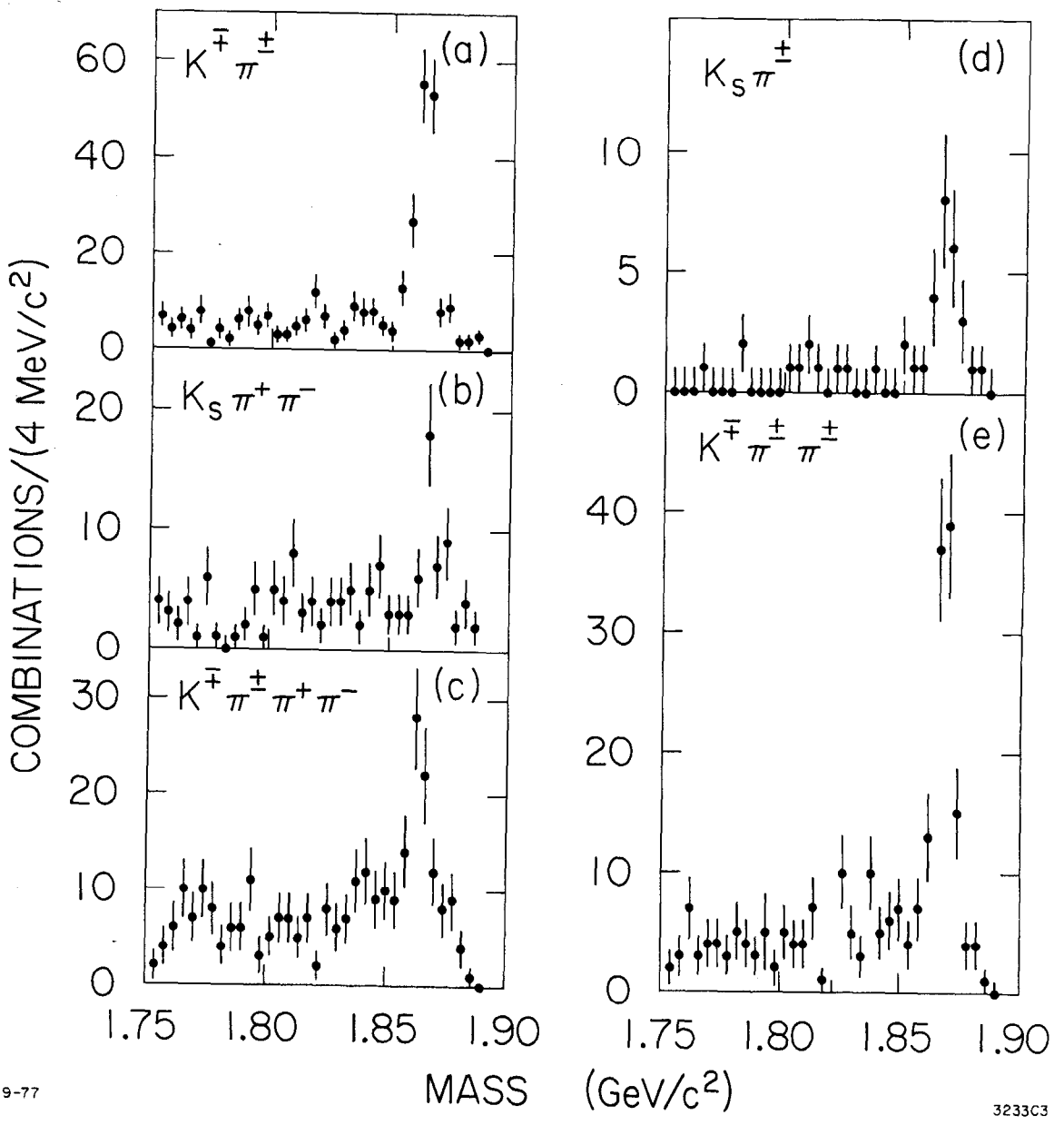
$K^{\mp}\pi^{\pm}$ (a)
$K_S\pi^+\pi^-$ (b)
$K^{\mp}\pi^{\pm}\pi^+\pi^-$ (c)
$K_S\pi^{\pm}$ (d)
$K^{\mp}\pi^{\pm}\pi^{\pm}$ (e)
COMBINATIONS/(4 MeV/c²)
MASS (GeV/c²)
9-77
3233C3

Fig. 2

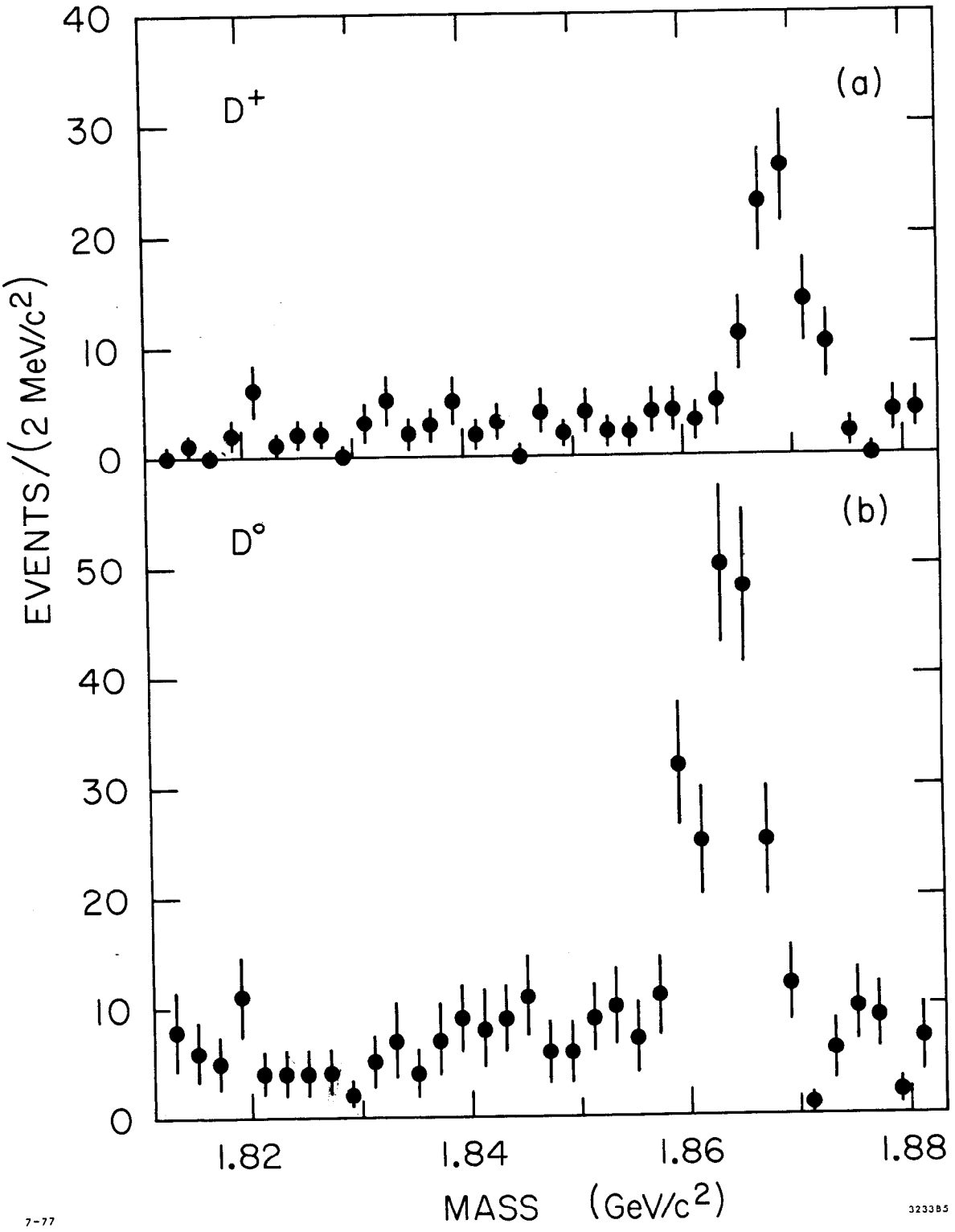
40
30
20
10
0
D+
(a)
EVENTS/(2 MeV/c2)
50
40
30
20
10
0
D°
(b)
1.82
1.84
1.86
1.88
MASS (GeV/c2)
7-77
3233B5

Fig. 3

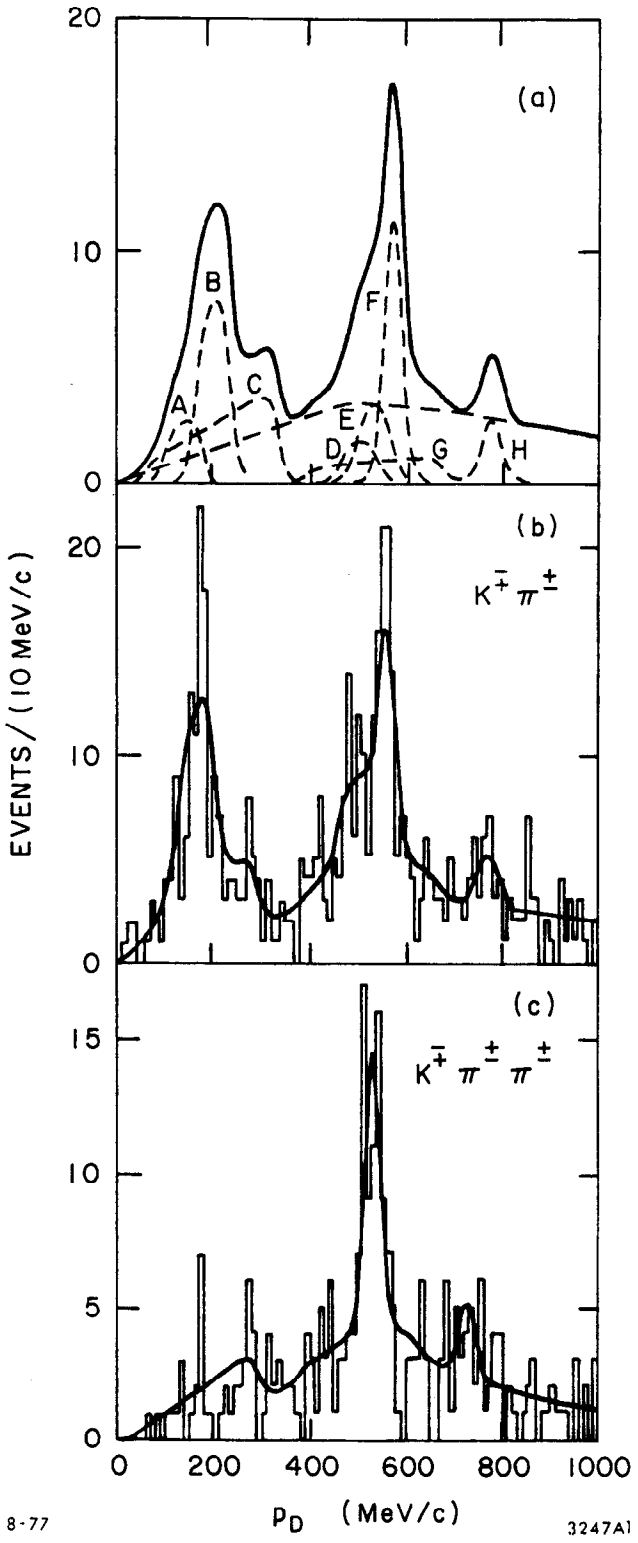
(a)
A
B
C
D
E
F
G
H
(b)
$K^{\mp}\pi^{\pm}$
(c)
$K^{\mp}\pi^{\pm}\pi^{\pm}$
EVENTS/(10 MeV/c)
p_D (MeV/c)
0
200
400
600
800
1000
8-77
3247A1

Fig. 4

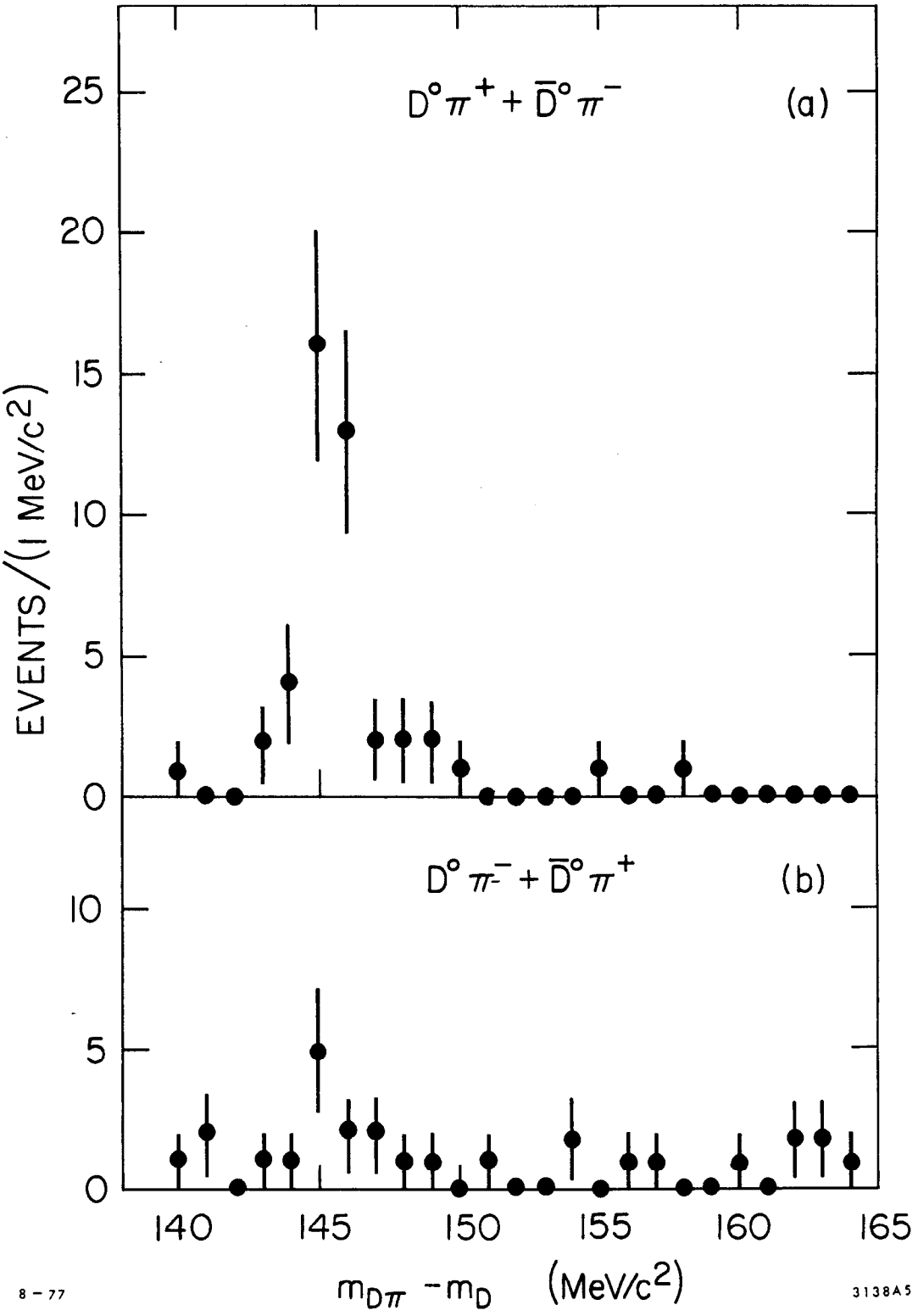
$D^\circ\pi^+ + \bar{D}^\circ\pi^-$
(a)
$D^\circ\pi^- + \bar{D}^\circ\pi^+$
(b)
EVENTS/(1 MeV/c²)
25
20
15
10
5
0
10
5
0
140
145
150
155
160
165
$m_{D\pi} - m_D$ (MeV/c²)
8-77
3138A5

Fig. 5

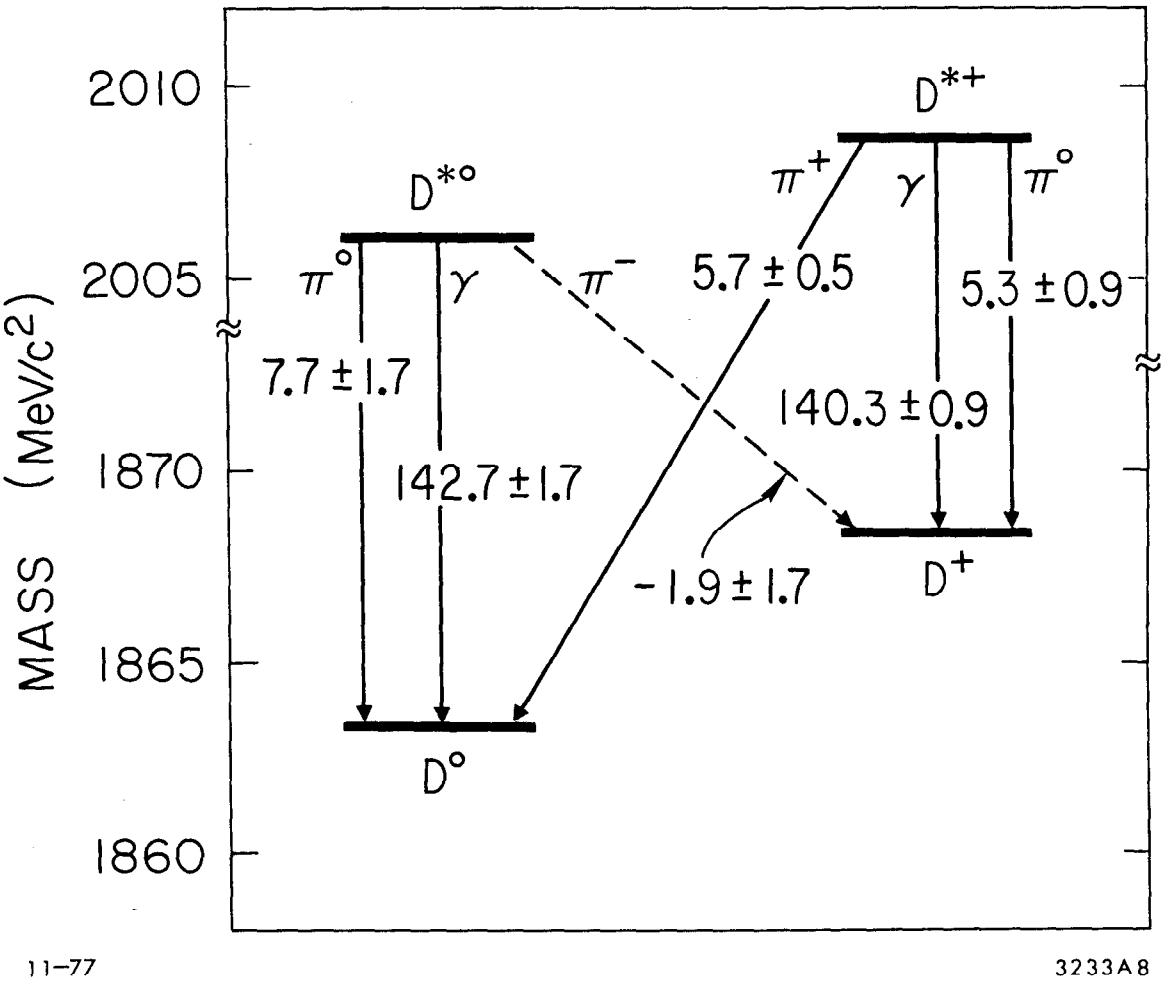
2010
2005
1870
1865
1860
MASS (MeV/c²)
D*°
D°
D*+
D+
π°
γ
π⁻
π⁺
γ
π°
7.7 ± 1.7
142.7 ± 1.7
5.7 ± 0.5
-1.9 ± 1.7
140.3 ± 0.9
5.3 ± 0.9
11-77
3233A8

Fig. 6

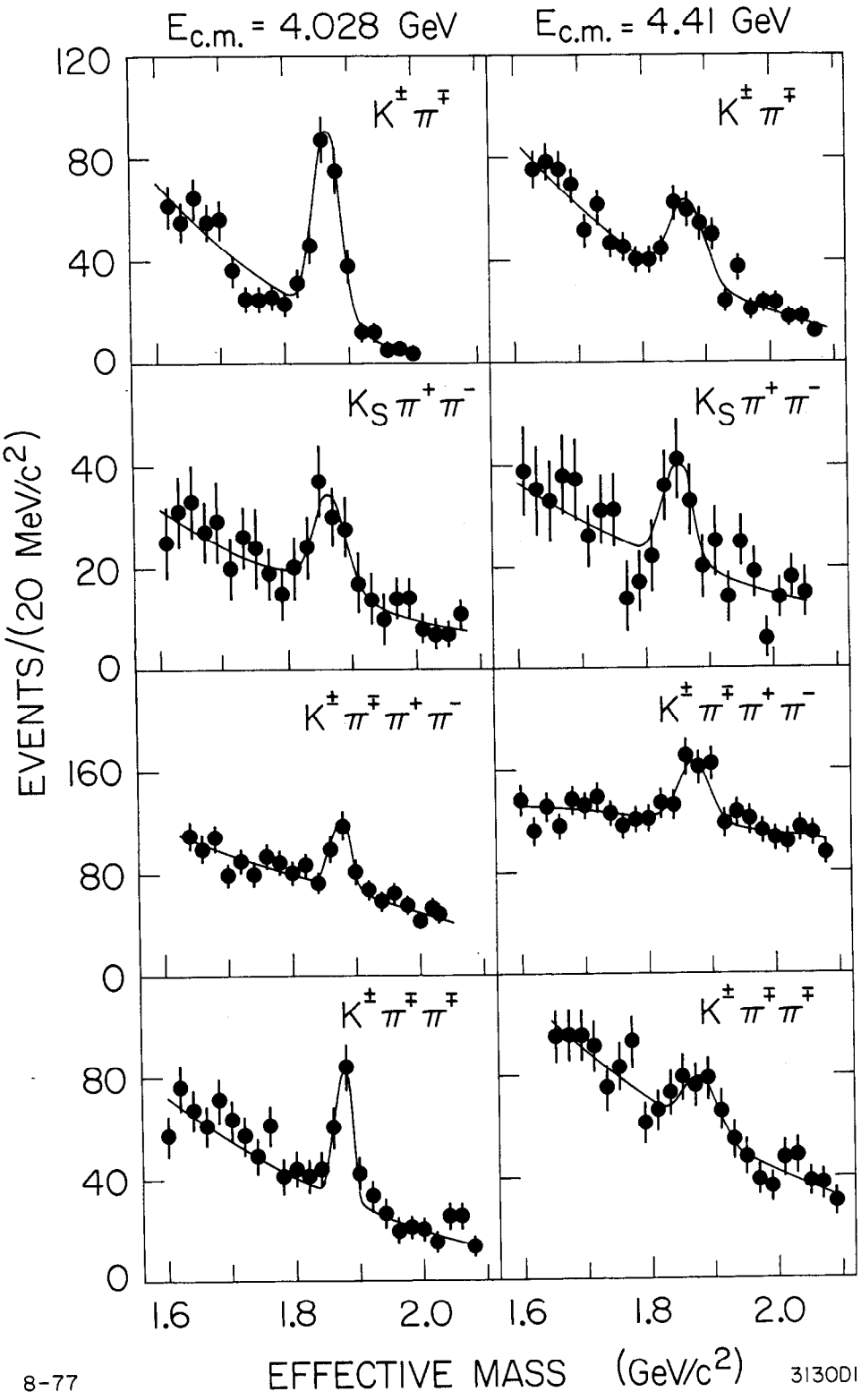
E c.m. = 4.028 GeV
E c.m. = 4.41 GeV
K± π∓
K± π∓
KS π+ π-
KS π+ π-
K± π∓ π+ π-
K± π∓ π+ π-
K± π∓ π∓
K± π∓ π∓
EVENTS/(20 MeV/c2)
EFFECTIVE MASS (GeV/c2)
8-77
313001

Fig. 7

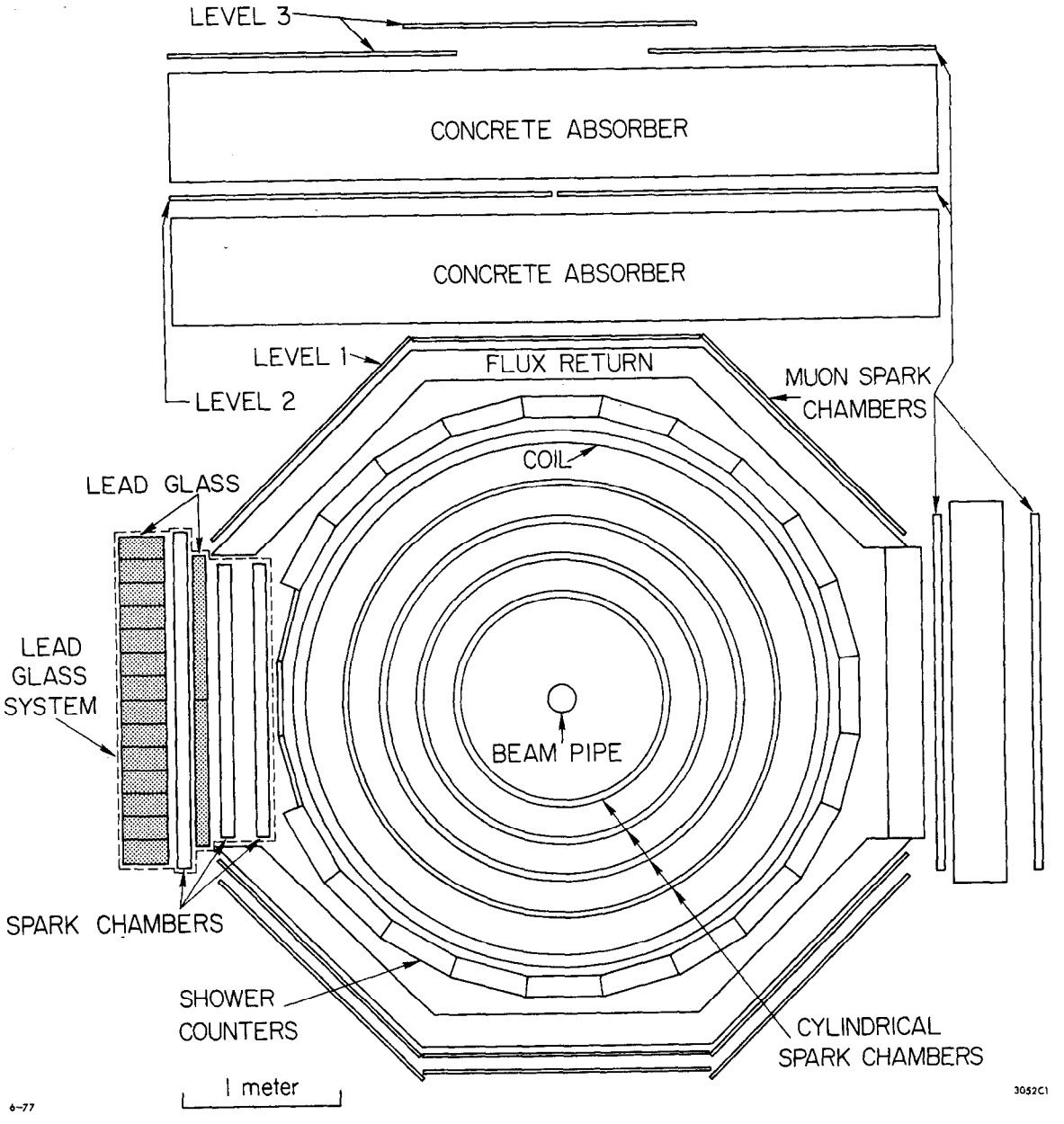
LEVEL 3
CONCRETE ABSORBER
CONCRETE ABSORBER
LEVEL 1
FLUX RETURN
MUON SPARK CHAMBERS
LEVEL 2
COIL
LEAD GLASS
LEAD GLASS SYSTEM
BEAM PIPE
SPARK CHAMBERS
SHOWER COUNTERS
CYLINDRICAL SPARK CHAMBERS
1 meter
6-77
3052C1

Fig. 8

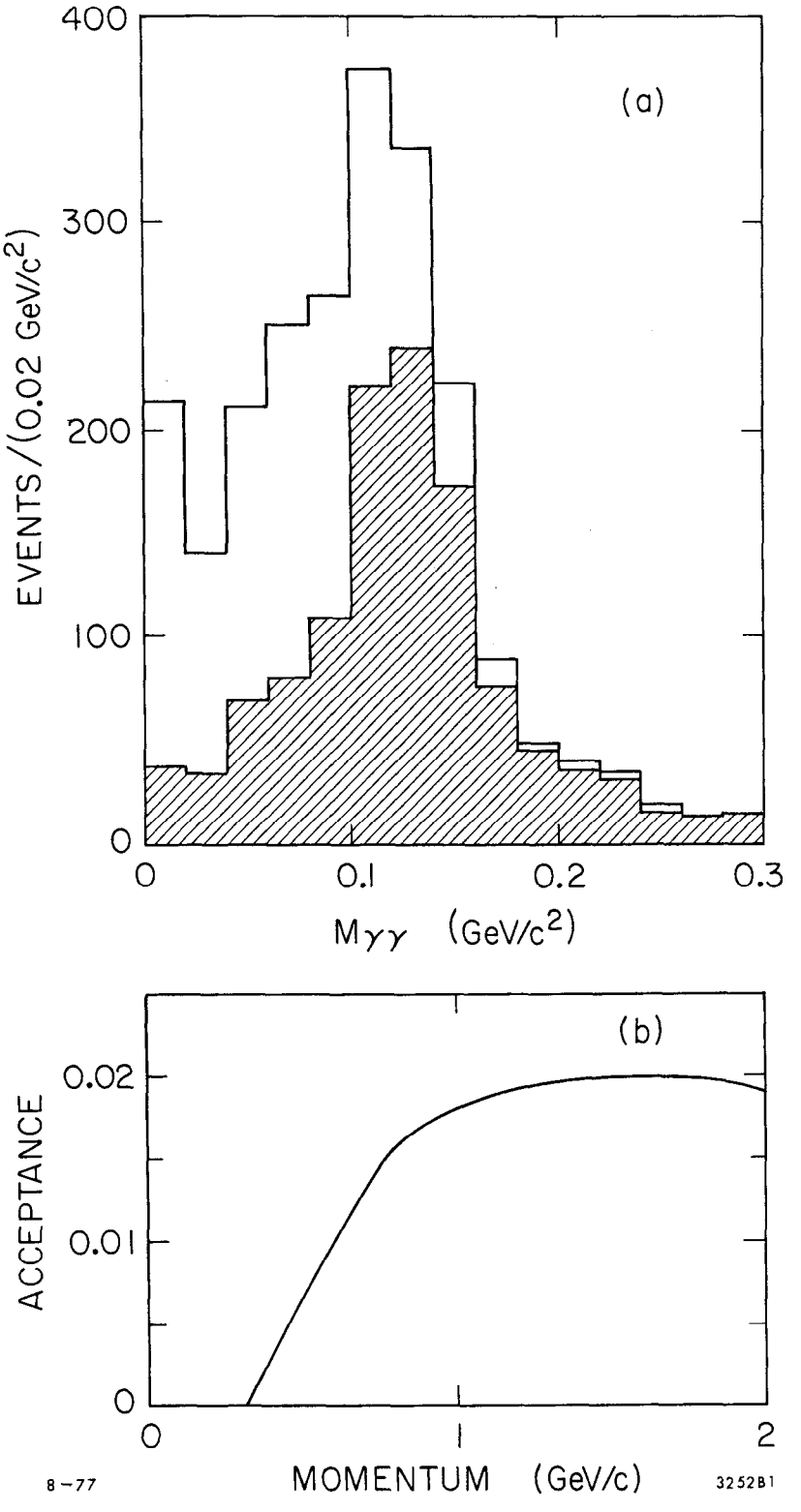
400
300
200
100
0
EVENTS/(0.02 GeV/c²)
(a)
0
0.1
0.2
0.3
Mγγ (GeV/c²)
(b)
0.02
0.01
0
ACCEPTANCE
0
1
2
MOMENTUM (GeV/c)
8-77
3252B1

Fig. 9

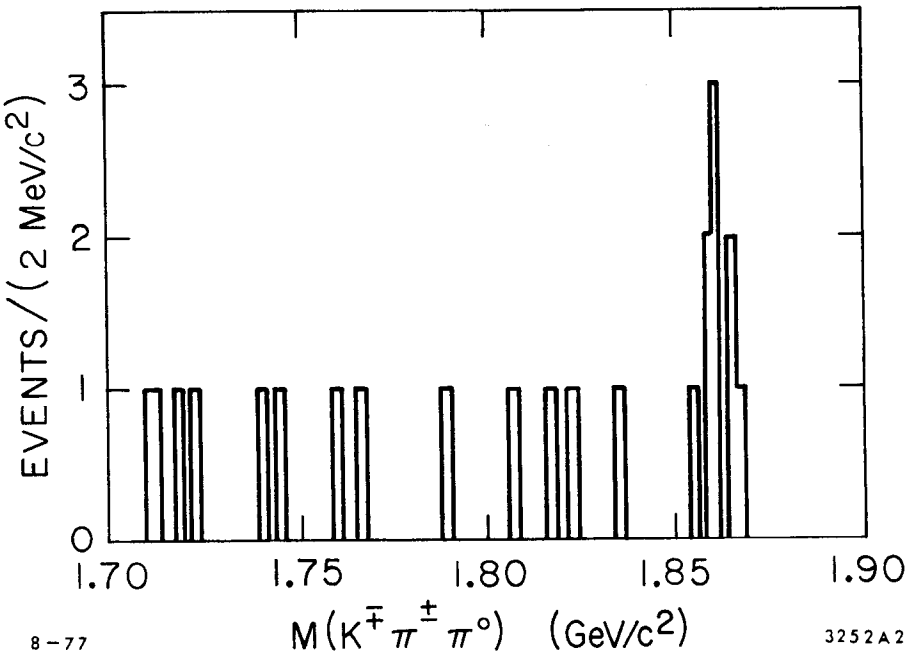

Fig. 10

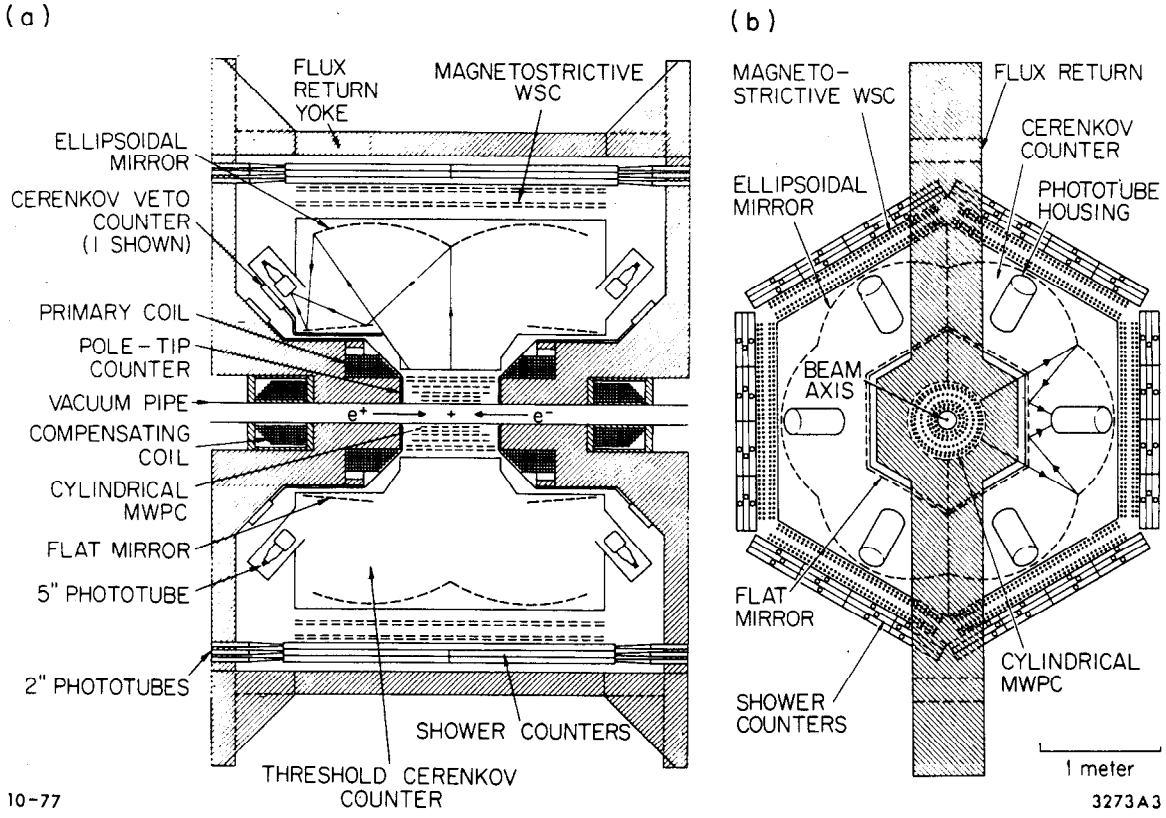
(a)
FLUX RETURN YOKE
MAGNETOSTRICTIVE WSC
ELLIPSOIDAL MIRROR
CERENKOV VETO COUNTER (1 SHOWN)
PRIMARY COIL
POLE-TIP COUNTER
VACUUM PIPE
e+
e-
COMPENSATING COIL
CYLINDRICAL MWPC
FLAT MIRROR
5" PHOTOTUBE
2" PHOTOTUBES
SHOWER COUNTERS
THRESHOLD CERENKOV COUNTER
10-77
(b)
MAGNETO-STRICTIVE WSC
FLUX RETURN
CERENKOV COUNTER
ELLIPSOIDAL MIRROR
PHOTOTUBE HOUSING
BEAM AXIS
FLAT MIRROR
CYLINDRICAL MWPC
SHOWER COUNTERS
1 meter
3273A3

Fig. 11

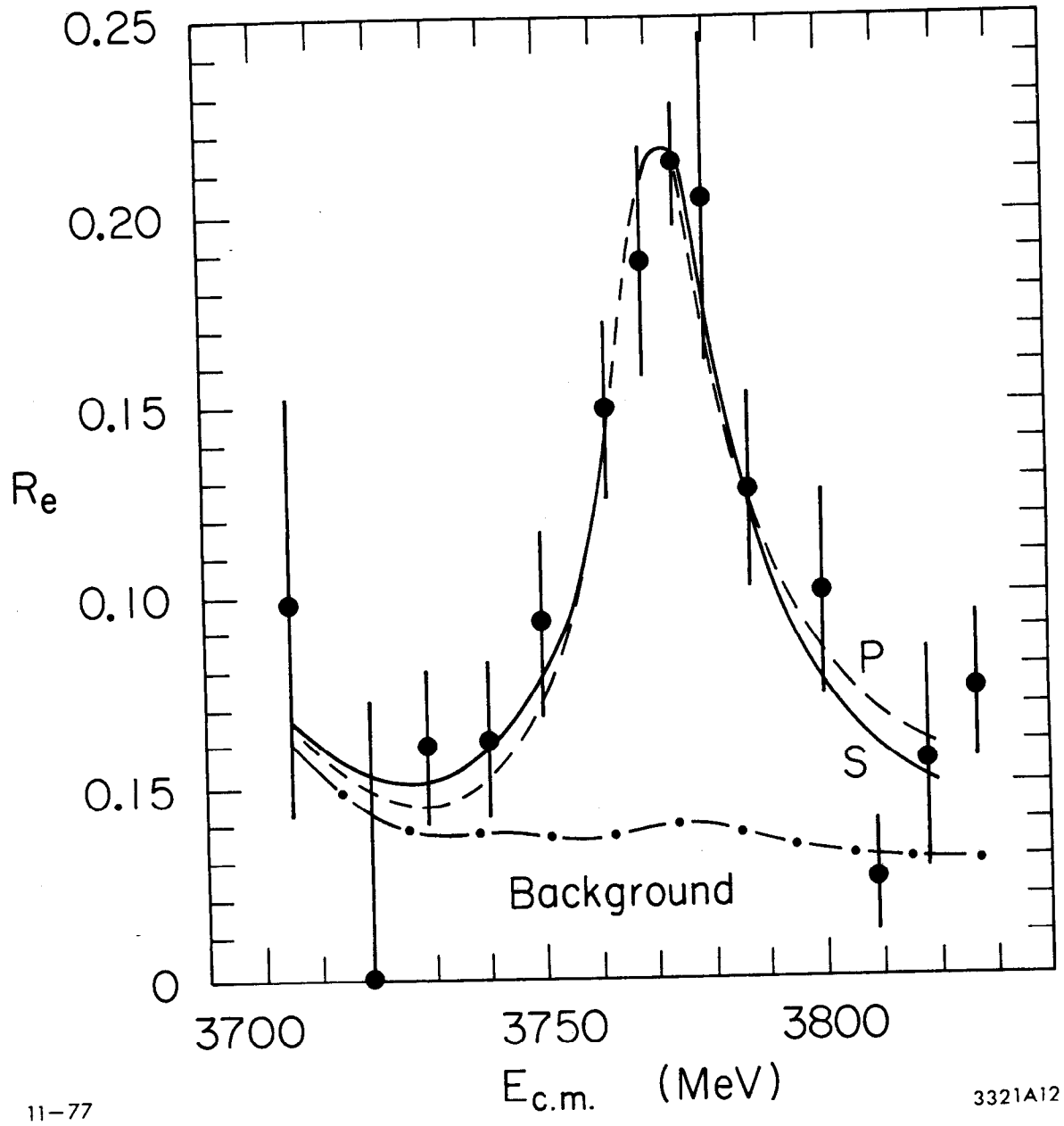
0.25
0.20
0.15
0.10
0.15
0
R_e
P
S
Background
3700
3750
3800
$E_{c.m.}$ (MeV)
11-77
3321A12

Fig. 12

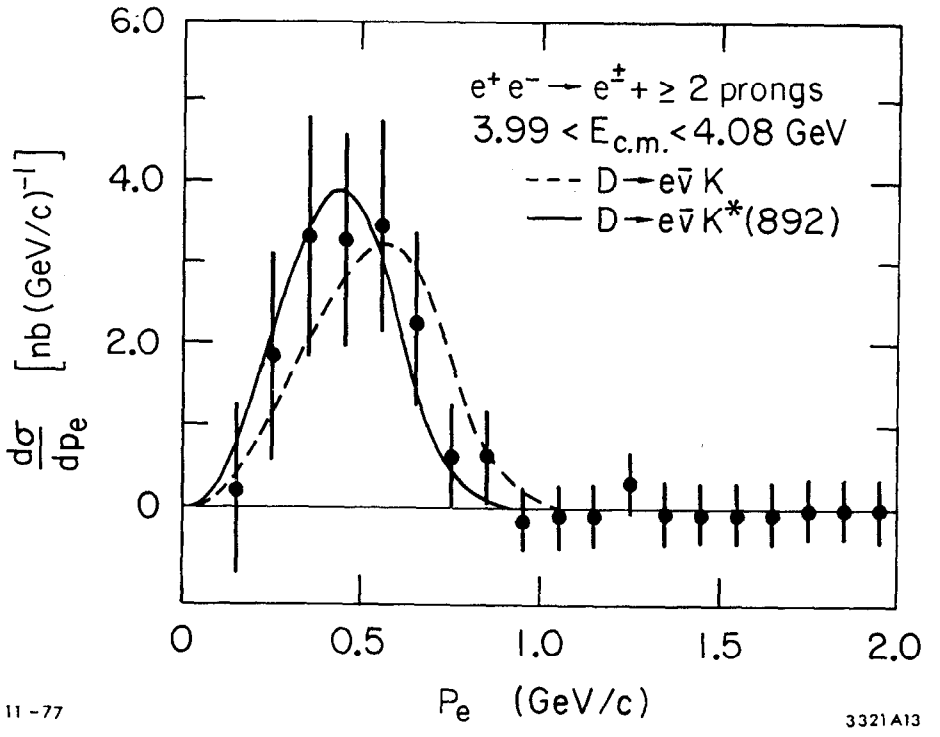
6.0
4.0
2.0
0
0
0.5
1.0
1.5
2.0
$e^+e^- \to e^\pm +$ ≥ 2 prongs
$3.99 < E_{c.m.} < 4.08$ GeV
--- $D \to e\bar{\nu}K$
— $D \to e\bar{\nu}K^*(892)$
$\frac{d\sigma}{dp_e}$ [nb (GeV/c)$^{-1}$]
P_e (GeV/c)
11-77
3321A13

Fig. 13

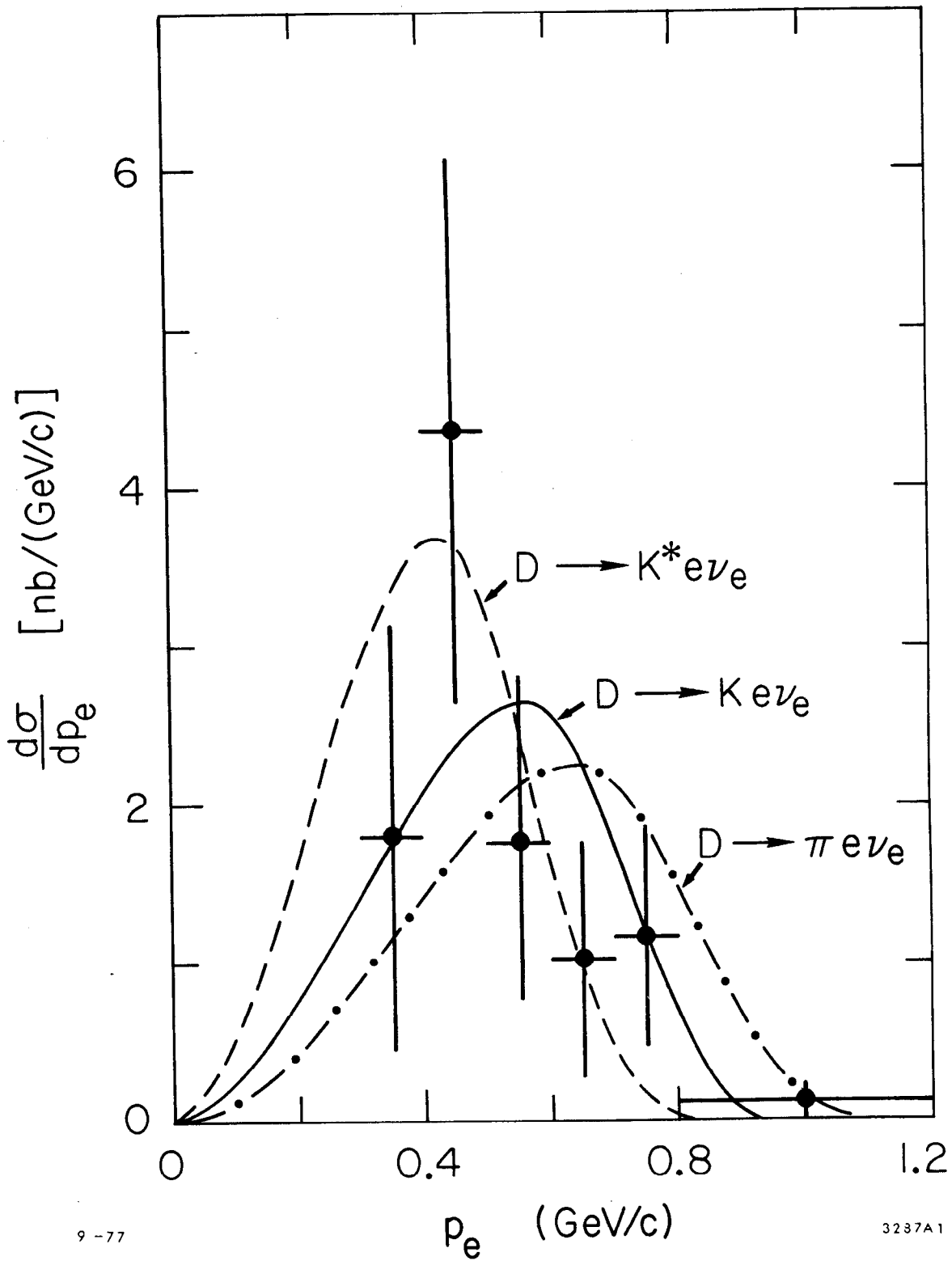
6
4
2
0
0
0.4
0.8
1.2
$\frac{d\sigma}{dp_e}$ [nb/(GeV/c)]
p_e (GeV/c)
D → K*eν_e
D → K eν_e
D → π eν_e
9-77
3237A1

Fig. 14

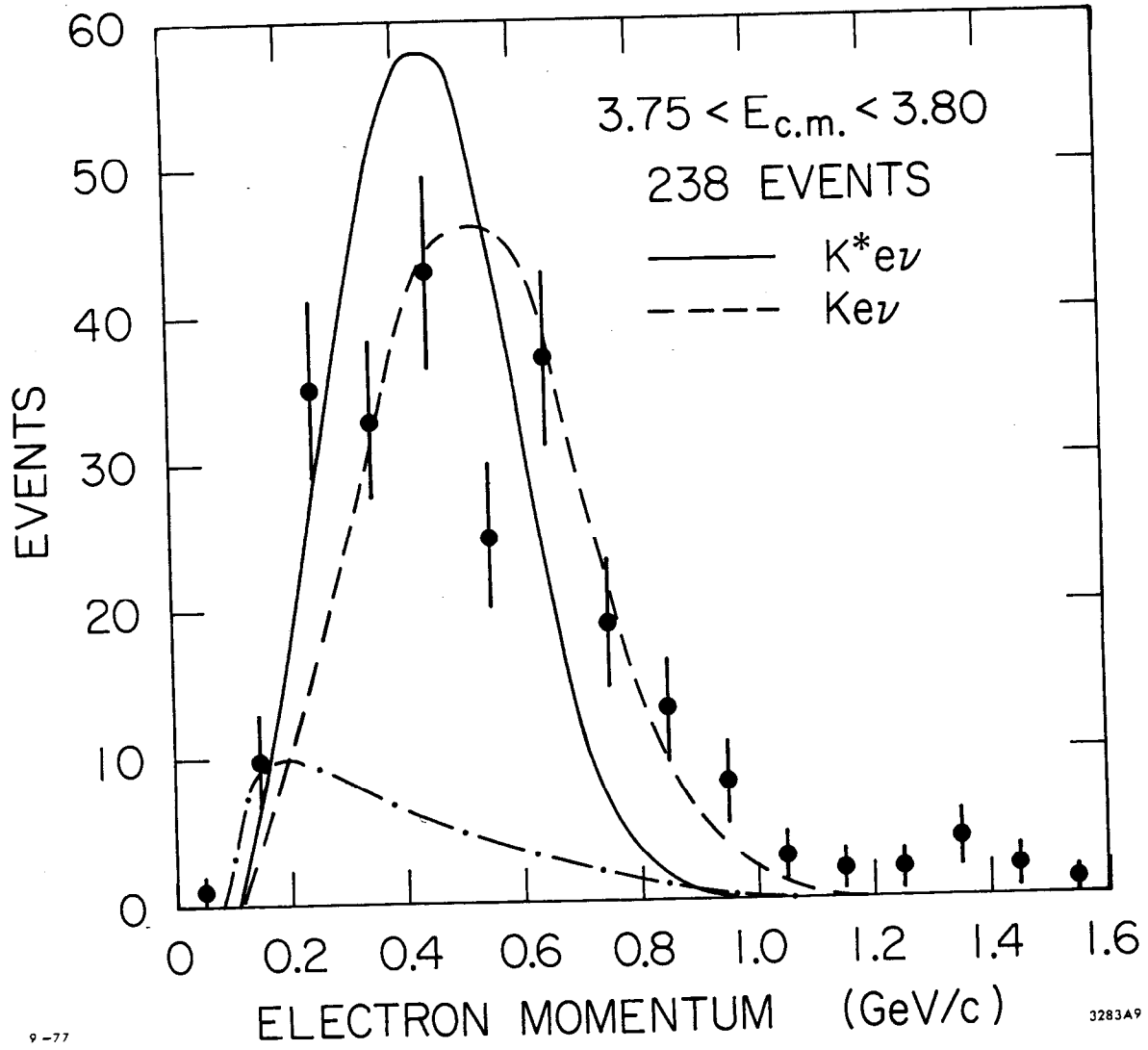
60
50
40
30
20
10
0
EVENTS
3.75 < E c.m. < 3.80
238 EVENTS
K*eν
Keν
0
0.2
0.4
0.6
0.8
1.0
1.2
1.4
1.6
ELECTRON MOMENTUM (GeV/c)
9-77
3283A9

Fig. 15

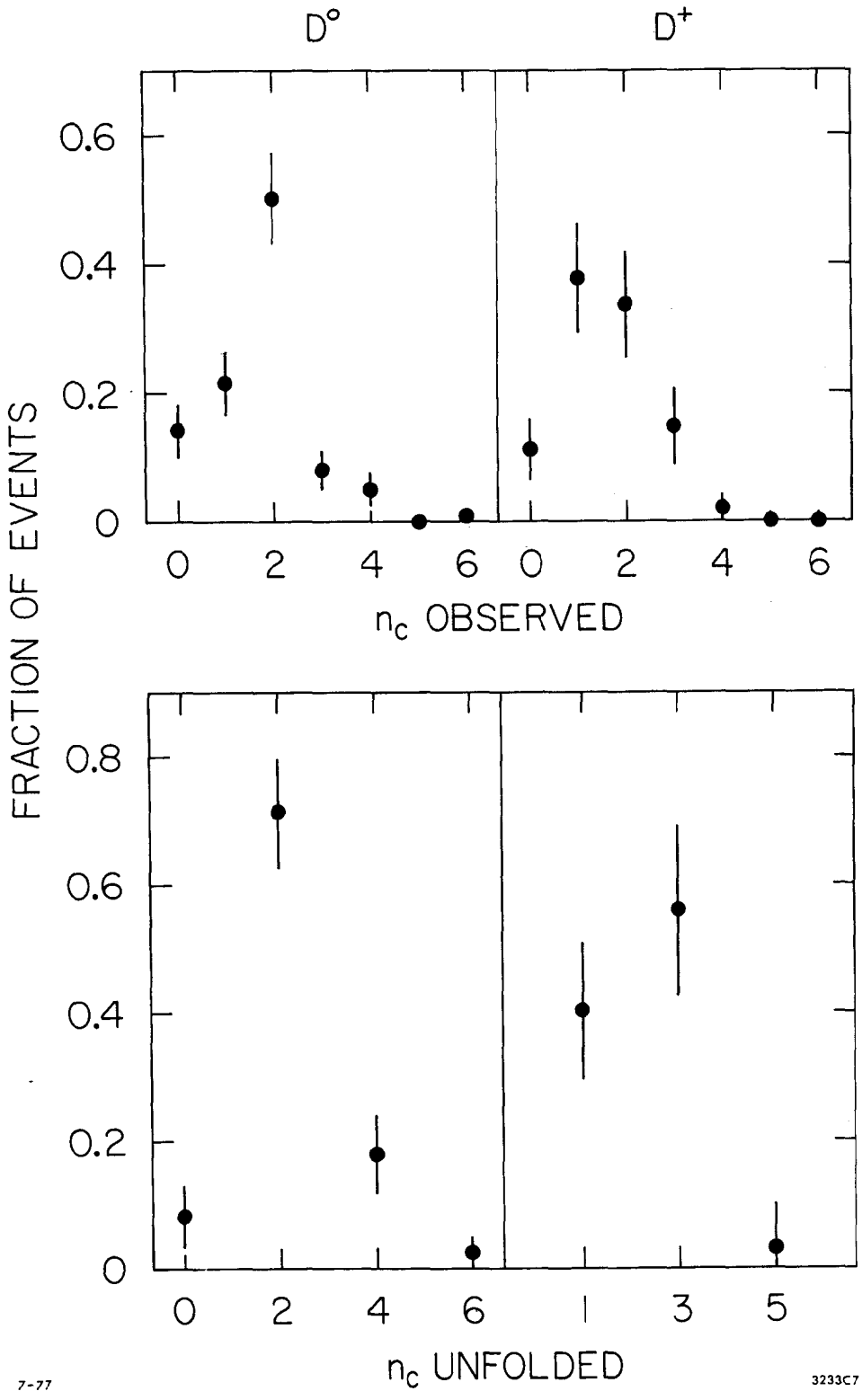
D°
D+
0.6
0.4
0.2
0
FRACTION OF EVENTS
0 2 4 6 0 2 4 6
n_c OBSERVED
0.8
0.6
0.4
0.2
0
0 2 4 6 1 3 5
n_c UNFOLDED
7-77
3233C7

Fig. 16

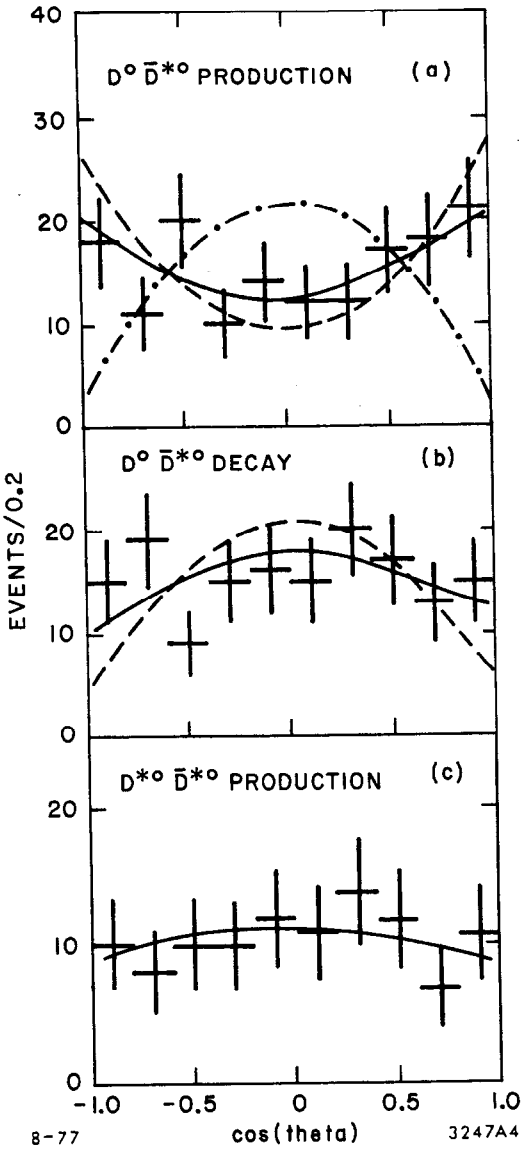
D° D̄*° PRODUCTION (a)
D° D̄*° DECAY (b)
D*° D̄*° PRODUCTION (c)
EVENTS/0.2
40
30
20
10
0
-1.0
-0.5
0
0.5
1.0
cos(theta)
8-77
3247A4

Fig. 17

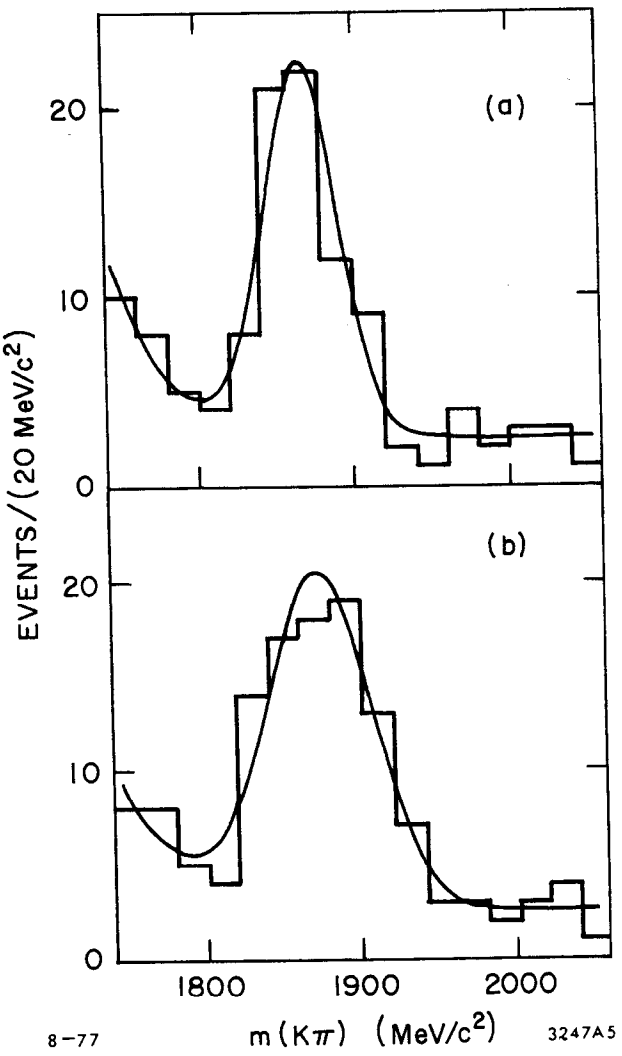
(a)
(b)
20
10
0
20
10
0
EVENTS/(20 MeV/c²)
1800
1900
2000
m(Kπ) (MeV/c²)
8-77
3247A5

Fig. 18

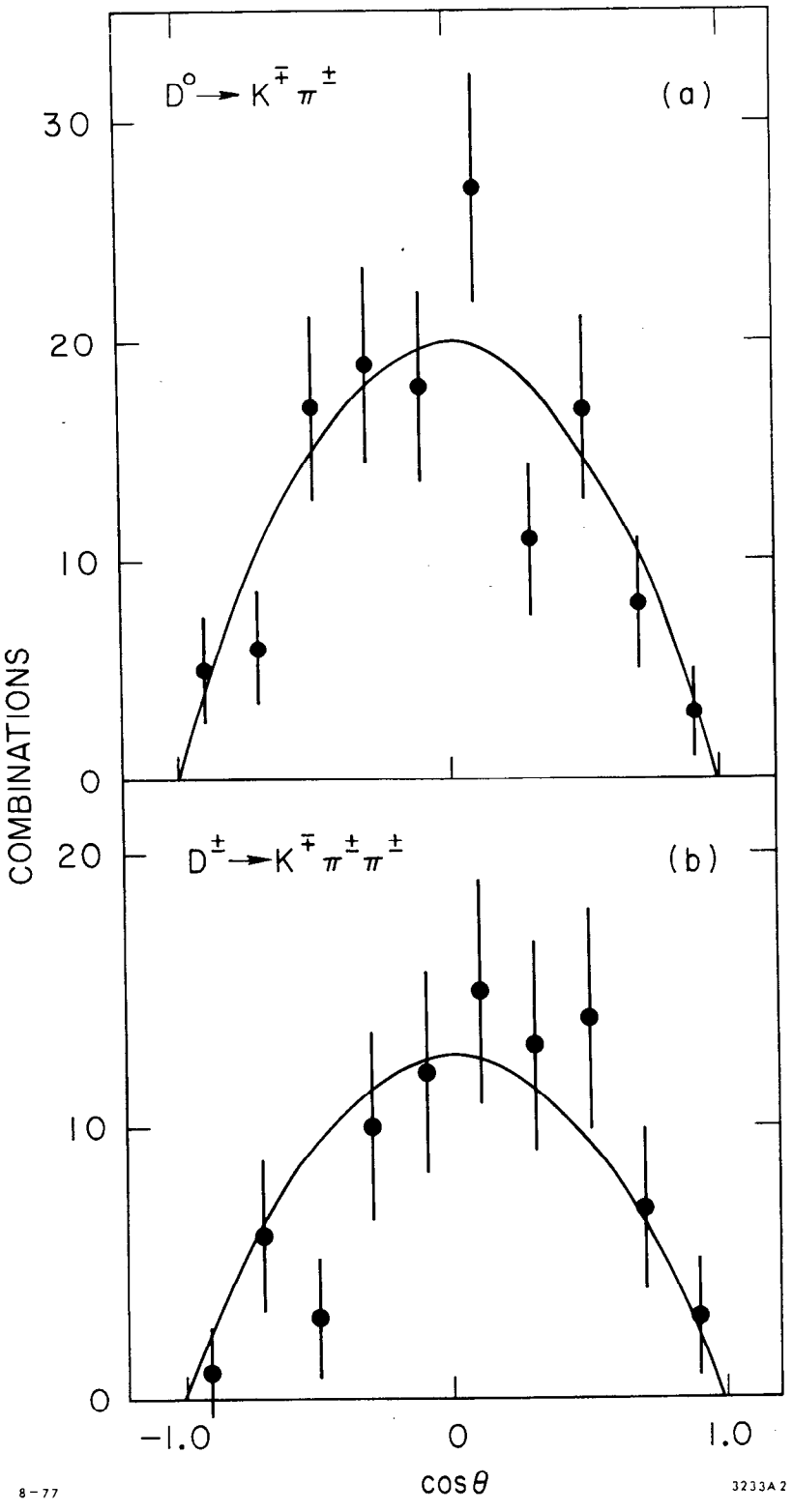
$D^0 \rightarrow K^{\mp}\pi^{\pm}$
(a)
30
20
10
0
COMBINATIONS
$D^{\pm} \rightarrow K^{\mp}\pi^{\pm}\pi^{\pm}$
(b)
20
10
0
-1.0
0
1.0
$\cos\theta$
8-77
3233A2

Fig. 19

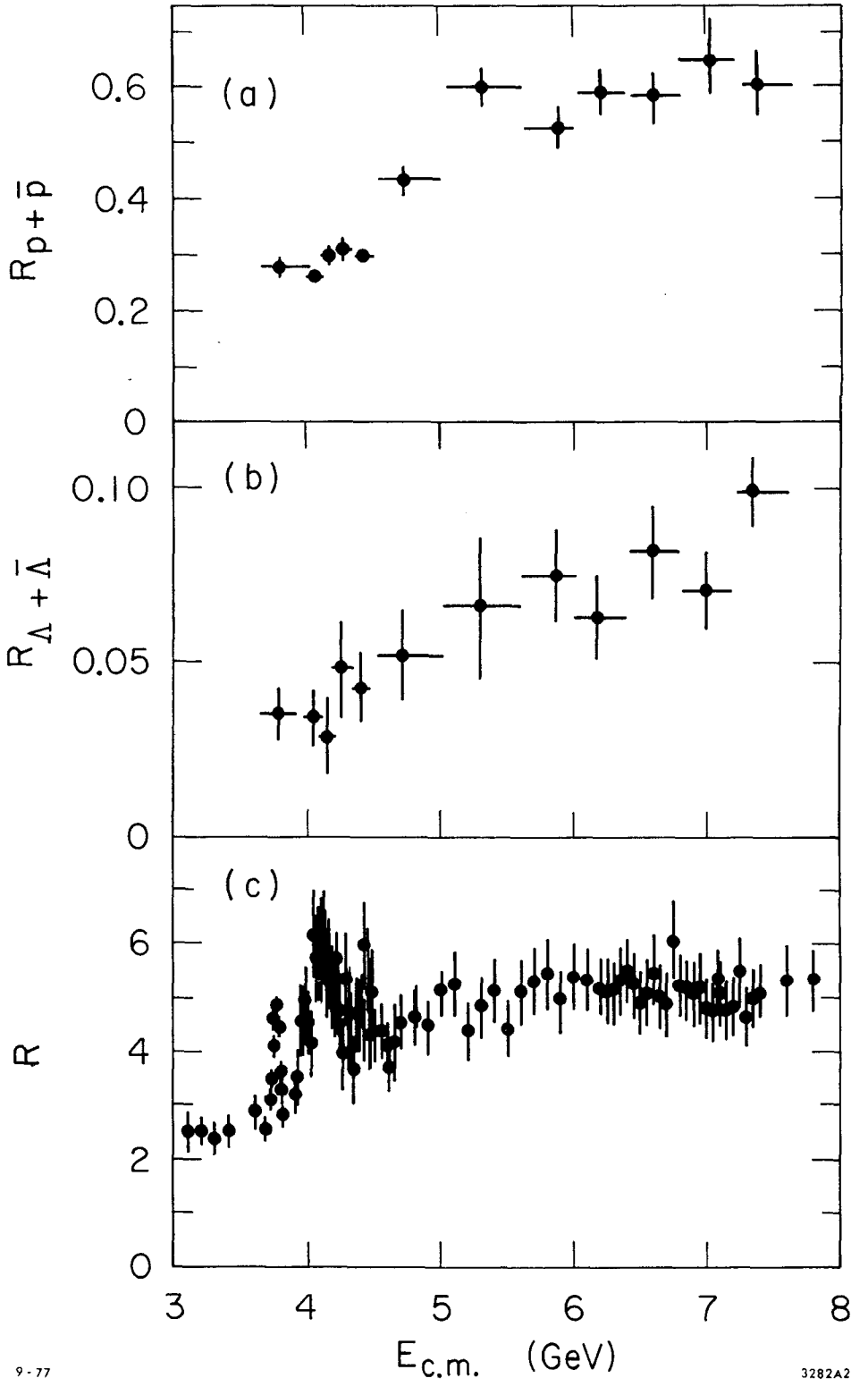
(a)
(b)
(c)
$R_{p+\bar{p}}$
$R_{\Lambda+\bar{\Lambda}}$
R
0.6
0.4
0.2
0
0.10
0.05
0
6
4
2
0
3
4
5
6
7
8
$E_{c.m.}$ (GeV)
9-77
3282A2

Fig. 20